This is an open access article published under a Creative Commons Non-Commercial No Derivative Works (CC-BY-NC-ND) Attribution License, which permits copying and redistribution of the article, and creation of adaptations, all for non-commercial purposes.

ACS AUTHORCHOICE

ACS Infectious Diseases

pubs.acs.org/journal/aidcbc

Article

Disruption of the *Plasmodium falciparum* Life Cycle through Transcriptional Reprogramming by Inhibitors of Jumonji Demethylases

Krista A. Matthews, Kossi M. Senagbe, Christopher Nötzel, Christopher A. Gonzales, Xinran Tong, Filipa Rijo-Ferreira, Natarajan V. Bhanu, Celia Miguel-Blanco, Maria Jose Lafuente-Monasterio, Benjamin A. Garcia, Björn F. C. Kafsack, and Elisabeth D. Martinez*,▽

Cite This: *ACS Infect. Dis.* 2020, 6, 1058−1075

Read Online

ACCESS | Metrics & More | Article Recommendations | Supporting Information

ABSTRACT: Little is known about the role of the three Jumonji C (JmjC) enzymes in *Plasmodium falciparum* (*Pf*). Here, we show that JIB-04 and other established inhibitors of mammalian JmjC histone demethylases kill asexual blood stage parasites and are even more potent at blocking gametocyte development and gamete formation. In late stage parasites, JIB-04 increased levels of trimethylated lysine residues on histones, suggesting the inhibition of *P. falciparum* Jumonji demethylase activity. These epigenetic defects coincide with deregulation of invasion, cell motor, and sexual development gene programs, including gene targets coregulated by the PfAP2-I transcription factor and chromatin-binding factor, PfBDP1. Mechanistically, we demonstrate that PfJmj3 converts 2-oxoglutarate to succinate in an iron-dependent manner consistent with mammalian Jumonji enzymes, and this catalytic activity is inhibited by JIB-04 and other Jumonji inhibitors. Our pharmacological studies of Jumonji activity in the malaria parasite provide evidence that inhibition of these enzymatic activities is detrimental to the parasite.

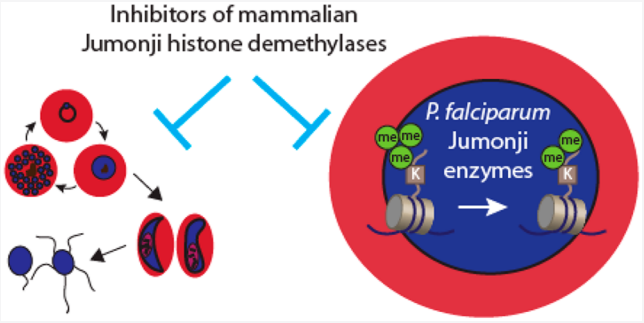

KEYWORDS: *malaria, Plasmodium falciparum, demethylases, Jumonji inhibitors, JIB-04, transcriptional reprogramming, gametocytes*

The most lethal of the five species of malaria is *Plasmodium falciparum* (*Pf*), affecting 3.4 billion humans annually.[1] The *P. falciparum* life cycle consists of single rounds of replication in the mosquito and human liver followed by the release of merozoites into the bloodstream. Following red blood cell (RBC) invasion by the extracellular merozoites, the asexual blood stages initiate remodeling of their host cell (ring forms and early trophozoite) followed by repeated rounds of nuclear replication (late trophozoite/early schizont) and a single round of cell division (schizont) ending with the release of new merozoites from the infected RBC 48 h later. A low percentage of schizonts form merozoites that are committed to differentiate into male and female sexual stage gametocytes that mediate transmission to the next host. Proper transcriptional regulation at each stage of *P. falciparum* development is essential for the successful completion of the life cycle.[2] *P. falciparum* controls several key gene expression programs through epigenetic mechanisms mediated by histone modifying enzymes. The trimethylation of histones at specific genomic loci regulates the expression of stage-specific transcription factors such as AP2-G, of nutrient uptake channels including the *clag3* gene paralogs, of invasion pathways, and of multigene families involved in antigenic variation.[2−11]

Histone trimethylation is regulated by trimethyl writers (including SET enzymes) and trimethyl erasers. Jumonji C domain (JmjC) containing enzymes, a subfamily of 2-oxoglutarate (2-OG)-dependent oxygenases that catalyze hydroxylation and demethylation of substrates, are the known demethylases of histone trimethylation (reviewed in ref 12). The core of the JmjC domain is comprised of a double-stranded β-helix fold containing the active site residues that coordinate Fe(II), bind 2-OG, and interact with substrates like histone tails.[12,13] The binding of Fe(II) and 2-OG initiates the oxidative decarboxylation of 2-OG, generating succinate and an iron intermediate. Jumonji enzymes use this intermediate to either hydroxylate or demethylate a variety of protein and nonprotein substrates. In contrast to the large

Received: November 22, 2019
Published: April 9, 2020

© 2020 American Chemical Society

https://dx.doi.org/10.1021/acsinfecdis.9b00455
ACS Infect. Dis. 2020, 6, 1058−1075

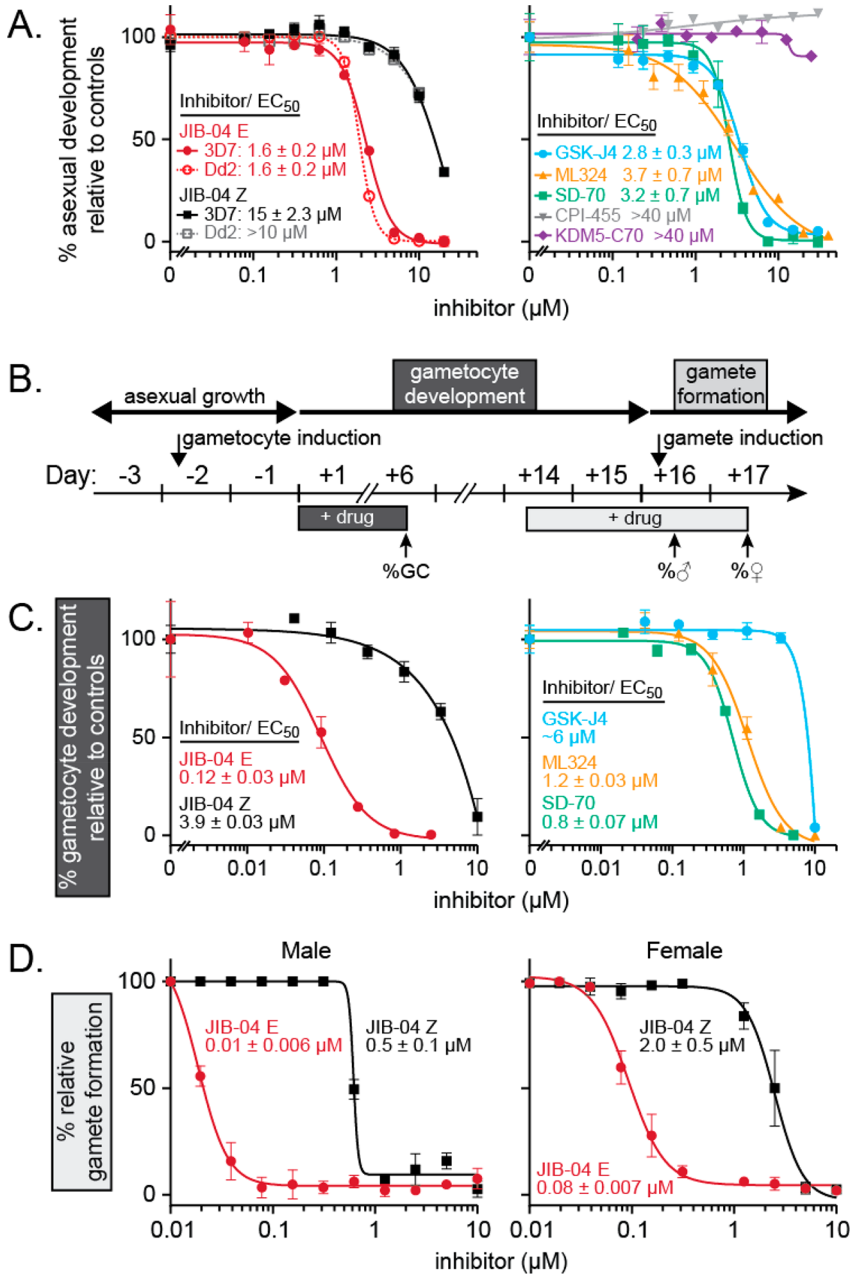

Figure 1. Jumonji inhibitors are active against asexual erythrocytic growth and potently block *P. falciparum* gametocyte development and gamete formation. Representative Jumonji inhibitor concentration curves against (A) asexual development, (C) gametocyte development, and (D) gamete formation. (A) 3D7 (solid line) or Dd2 (dashed line) asexual parasites synchronized to rings were treated with JIB-04 E (red circles) and Z (black squares) isomers (left panel) or GSK-J4 (cyan circles), ML324 (orange triangles), SD-70 (green squares), CPI-455 (gray inverted triangles), and KDM5-C70 (purple diamonds) (right panel). Asexual development was measured using the standard 3 day growth assay as described in the Materials and Methods and is presented as a percent of vehicle-treated controls. (B) Schematic of gametocyte and gamete induction relative to inhibitor exposure. Synchronized asexual parasites were cultured at high parasitemia on day −2 to induce gametocytogenesis. For the development assays (dark gray boxes), gametocytes were exposed to the inhibitor starting on day +1 through day +6. Parasitemia (%PT) and gametocytemia (% GC) were measured by flow cytometry as described in the Materials and Methods. For gamete formation assays (light gray boxes), inhibitor was added to stage V gametocytes for 48 h prior to induction on day +14. Male exflagellation (%♂) and female gamete formation (%♀) was measured on day +16 and day +17, respectively, as described in the Materials and Methods. (C) Representative concentration curves of JIB-04 E and Z (left panel) and other Jumonji inhibitors (right panel) against gametocyte development relative to vehicle controls. (D) Representative concentration curves of JIB-04 E and Z against male (left panel) and female (right panel) gamete formation relative to vehicle controls. Nonlinear regression curves ([inhibitor] vs response − variable slope (four parameters)) were fit to the data using GraphPad Prism v8. Error bars represent the standard deviation of technical triplicates. EC_{50} concentrations (μM) are presented as mean ± SEM of the fitted inhibition curves from three or more independent experiments.

family of Jumonji enzymes in mammals (~30), the *P. falciparum* genome encodes only three proteins containing JmjC enzymatic domains, designated as PfJmjC1 (PF3D7_0809900), PfJmjC2 (PF3D7_0602800), and PfJmj3 (PF3D7_1122200).[14,15] The catalytic triad residues that coordinate Fe(II) (HxD/E,H) and the 2-OG-binding residues

https://dx.doi.org/10.1021/acsinfecdis.9b00455
ACS Infect. Dis. 2020, 6, 1058−1075

are conserved in all three *P. falciparum* proteins. Furthermore, all three *P. falciparum* Jumonji enzymes are expressed during the parasite's intraerythrocytic developmental cycle (IDC), during gametocyte development, and in ookinetes.[16−19] Jiang et al. generated single knockout lines of *PfJmjC1* and *PfJmjC2* that were viable, indicating that neither of these enzymes are essential for blood stage parasite survival in a laboratory environment.[15] *PfJmj3* has yet to be subjected to similar knockout analysis, although a recent transposon mutagenesis study suggests that an exonal insertion in the gene for *PfJmj3* yields viable parasites.[20] The essentiality of the Jumonji enzymes in other stages of the *P. falciparum*'s life cycle has yet to be investigated. In all organisms studied to date, Jumonji histone lysine demethylases (KDMs) are the only family of histone demethylases enzymatically capable of removing trimethyl marks; thus, the aggregate PfJmj histone demethylase activity is likely central in regulating transcriptional programs in the parasite.[12,21]

We and others have developed small molecule inhibitors of mammalian Jumonji KDM enzymes that interfere with catalysis by disrupting interactions with the iron cofactor, the 2-OG cosubstrate, and/or the histone substrate.[22−29] Since PfJmj proteins contain the conserved amino acid residues for binding to cofactor, cosubstrate, and substrate, we speculated that these inhibitors would block the total Jumonji catalytic activity in the parasite. We therefore evaluated the antimalarial activity of a collection of small molecule inhibitors of mammalian Jumonji KDM enzymes with a range of specificities against various subfamilies. We find that inhibitors of mammalian Jumonji KDMs arrest parasite development and trigger parasite death in replicating blood stages, and potently prevent gametocyte development and gamete formation. Furthermore, we show that three of the four small molecules inhibit conversion of 2-OG to succinate by recombinant PfJmj3. Consistent with the inhibition of malarial Jumonji KDMs, Jumonji inhibitors alter global levels of histone trimethylation in *P. falciparum*, resulting in the deregulation of the parasite's transcriptional developmental program and ultimately parasite death.

RESULTS

Inhibitors of Mammalian Jumonji Enzymes Have Antimalarial Activity against Drug Sensitive and Drug Resistant Asexual Blood Stage Parasites in Culture. The *Plasmodium falciparum* (*Pf*) genome encodes three proteins containing JmjC enzymatic domains, designated as PfJmjC1 (PF3D7_0809900), PfJmjC2 (PF3D7_0602800), and PfJmj3 (PF3D7_1122200) (Figure S1A). Residues in the mammalian Jumonji enzymes that are required for catalysis through iron and 2-oxoglutarate (2-OG) binding and for substrate binding are conserved in all three *P. falciparum* proteins (Figure S1B). Since several known inhibitors of mammalian Jumonji enzyme activity interfere with iron/2-OG/substrate binding, we evaluated these small molecules for antimalarial activity.[22−29] We first tested our own pan-selective inhibitor of Jumonji KDMs, JIB-04, in its active (E) and inactive (Z) isomeric forms since it is potent in culture and active *in vivo* against KDMs in cancer mammalian models (Table S1).[23] We measured the inhibition of blood stage asexual parasite growth using a standard 3 day assay in parasites synchronized to rings.[30] The JIB-04 E isomer blocked the viability of both drug-sensitive 3D7 as well as multidrug-resistant Dd2 parasites with an EC_{50} of 1.6 μM, while the inactive Z isomer was far less effective (EC_{50} > 10 μM) (Figures 1A, left panel, and S1C). To establish the generality of these findings, we then tested a panel of other known Jumonji inhibitors with various specificities for the mammalian enzymes (Table S1). GSK-J4, which preferentially inhibits H3K27me3 Jumonji KDMs in some model systems, also inhibited both 3D7 and Dd2 parasites while the less active isomer GSK-J5 did not (Figures 1A, right panel, and S1C,D).[23,27,31−33] ML324 and SD-70, reported to inhibit KMD4 Jumonji family members, were also active against 3D7 and Dd2 parasites (Figures 1A, right panel, and S1D).[34,35] Inhibitors known to selectively target the KDM5 subfamily of Jumonji enzymes such as CPI-455 and KDM5-C70 lacked antimalarial activity even at the highest doses tested (40 μM) (Figure 1A, right panel, and S1D).[26,29,36] Inhibition by JIB-04 E, GSK-J4, ML324, and SD-70, but not by CPI-455 or KDM5-C70, all active site inhibitors, suggests that effects on parasite growth are specific and not simply the result of general iron chelation or cytotoxicity against RBCs. Taken together, these studies establish that multiple Jumonji KDM inhibitors targeting mammalian enzymes other than only KDM5s are effective at blocking the viability of both drug-sensitive and drug-resistant blood stage *P. falciparum* parasites with similar potency.

Jumonji Inhibitors Disrupt Gametocyte Development and Gamete Formation. Next, we investigated the effects of Jumonji inhibitors on gametocyte (GC) development. Following sexual commitment, reinvaded ring stages were exposed to *N*-acetylglucosamine to kill asexual parasites and to Jumonji inhibitors for 6 days. Gametocytotemia was quantified by flow cytometry on day 6 (%GC) (Figure 1B; gametocyte development). JIB-04 E was highly effective in preventing gametocyte development as were SD-70 and ML324. Dose response studies determined that, among these Jumonji inhibitors, JIB-04 E is the most potent inhibitor of gametocyte development with an EC_{50} concentration of ∼120 nM, followed by SD-70 (∼800 nM) and ML324 (∼1 μM) (Figure 1C). GSK-J4 and the inactive Z isomer of JIB-04 were effective only at high doses (Figure 1C). Thus, while JIB-04, SD-70, and ML324 have 4−12-fold higher potency against these sexual stages than against asexual parasites, GSK-J4 loses potency.

We then assessed if JIB-04 had effects on gamete maturation using the dual gamete formation assay (Figure 1B; gamete formation).[37,38] We measured male gamete formation by exflagellation assays and female gamete formation by live cell staining with anti-Pfs25-Cy3 antibodies, a female-gamete specific marker.[39] JIB-04 E potently inhibited male exflagellation centers with an EC_{50} of ∼10 nM, while the inactive Z isomer had a much weaker effect (>500 nM) (Figure 1D, left panel). JIB-04 E also robustly blocked female gamete formation as measured by decreased Pfs25 protein, with EC_{50} values of ∼80 nM compared to >2 μM for the inactive Z isomer (Figure 1D, right panel). These results indicate that Jumonji inhibitors disrupt gametocyte development and gamete formation with high potency preferentially blocking male gamete formation.

Jumonji Inhibitors Delay Progression of Ring- or Trophozoite-Treated Asexual Blood Stage Parasites. To further characterize the mode of antimalarial action of Jumonji inhibitors, we treated parasites synchronized at specific blood form stages and evaluated the effects of drug exposure on subsequent progression through the intraerythrocytic developmental cycle (IDC). First, we treated rings with each inhibitor at its EC_{50} concentration and monitored parasite

https://dx.doi.org/10.1021/acsinfecdis.9b00455
ACS Infect. Dis. 2020, 6, 1058−1075

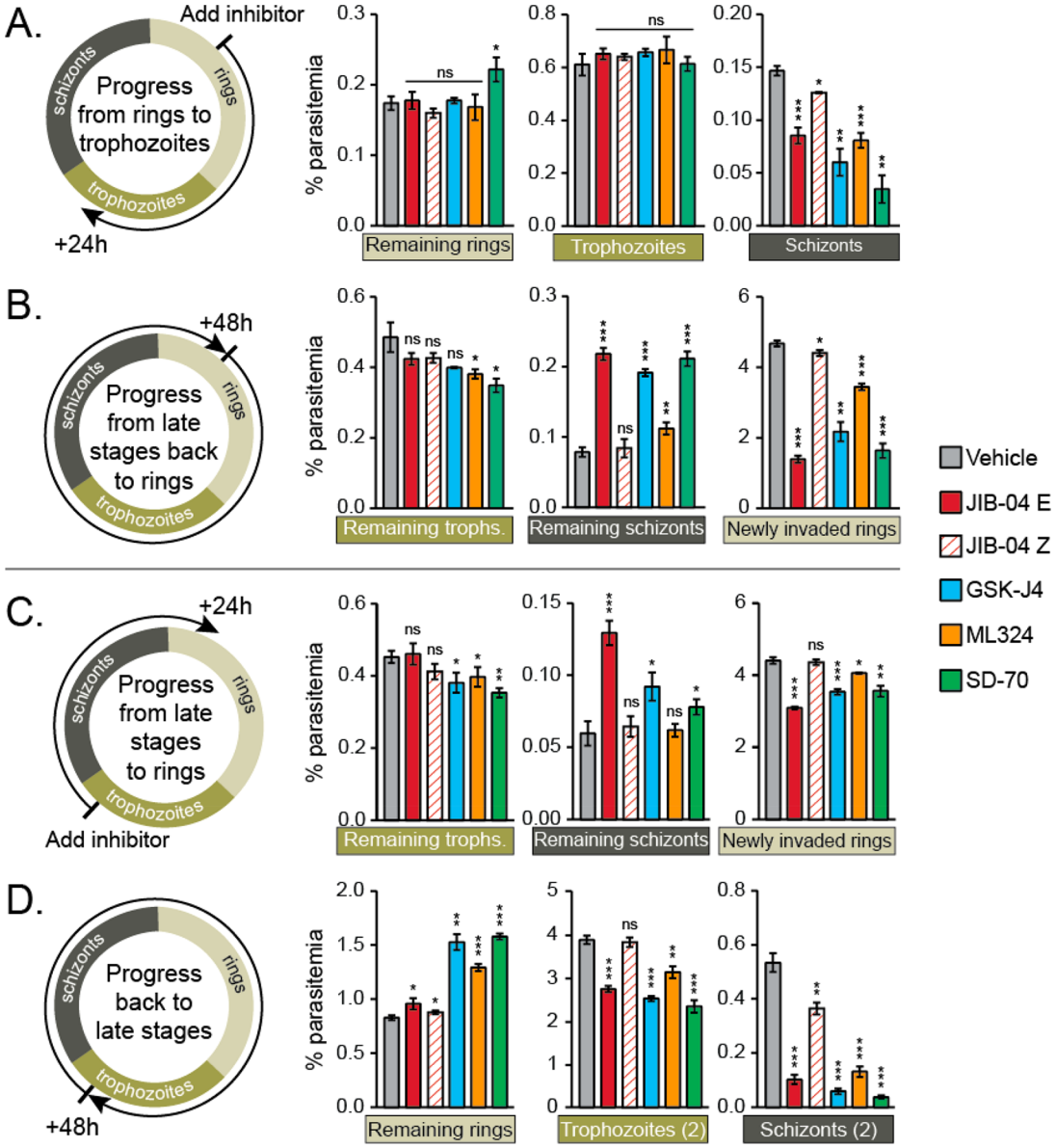

Figure 2. Exposure of ring or late stage asexual parasites to Jumonji inhibitors significantly impairs parasite development through IDC. Synchronized (A, B) ring parasites or (C, D) trophozoite parasites were grown in the presence of 1× EC_{50} concentrations of Jumonji inhibitors for 48 h. Quantification of parasite progression after 24 h exposure (A, C) and 48 h exposure (B, D) was monitored by flow cytometry and Giemsa stained thin blood smears as shown by the representative dot plots and images in Figure S3. Ring, trophozoite, and schizont parasites are gated as described in the Materials and Methods. Bar graphs present the mean ± SD of rings, trophozoites, and schizonts as % parasitemia of triplicate wells from one of two independent experiments. *p* values are calculated using a *t* test between vehicle- and inhibitor-treated samples. n.s., nonsignificant; *, $p < 0.05$; **, $p < 0.01$; ***, $p < 0.001$.

development 24 and 48 h post-exposure by flow cytometry (Figures 2A,B and S2A,B). After 24 h, about 65% of rings treated with vehicle had progressed to trophozoites and 15% to schizonts (Figures 2A and S2A). While some rings treated with JIB-04 E also progressed in the cell cycle, there were significantly fewer parasites entering schizogony (Figure 2A, schizonts). We observe a similar decrease in schizonts with GSK-J4, ML324, and SD-70, the other Jumonji inhibitors that showed antimalarial activity (Figures 2A and S2A). None of these inhibitors had any effect on total parasite numbers at this time point (Figure S2A).

After 48 h, ring parasite cultures treated with vehicle or the inactive Z isomer completed the IDC and reinvaded new RBCs, resulting in an increase in parasitemia from ∼1% to ∼5% (Figure S2B). In contrast to the controls, the treatment with Jumonji inhibitors markedly reduced total parasite numbers (Figure S2B). This reduction in parasitemia is mainly due to an increase in the number of remaining schizonts that have yet to complete the cell cycle, thus resulting in fewer newly invaded rings (Figures 2B and S2B). JIB-04 E-, GSK-J4-, and SD-70-treated cultures only had between ∼1.5% and 2% newly invaded ring parasites compared to ∼4.5% in the controls. Treatment with ML324 showed a more modest decrease in newly invaded rings (∼3.5% rings), consistent with the higher parasitemia of these cultures.

To investigate if late stage parasites were susceptible to Jumonji inhibitors, we next treated trophozoite parasites over 48 h and monitored progression through the remaining IDC

https://dx.doi.org/10.1021/acsinfecdis.9b00455
ACS Infect. Dis. 2020, 6, 1058−1075

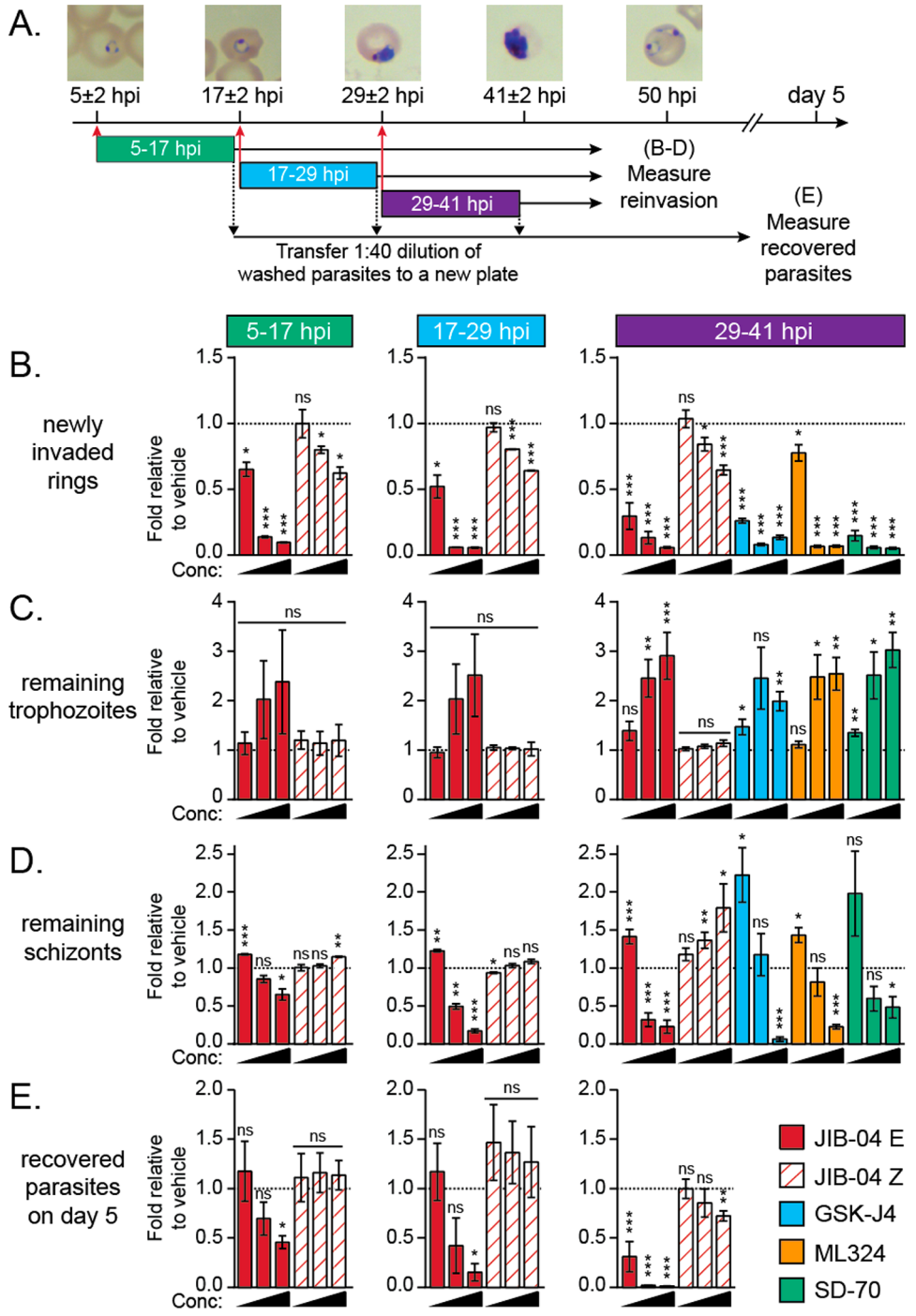

Figure 3. Transient exposure to JIB-04 E impairs development at all stages throughout the IDC with long-term consequences. (A) Schematic of the experimental setup. Tightly synchronized parasites were exposed to the vehicle or 1.5, 7.5, or 15 μM JIB-04 E (corresponding to 1×, 5×, or 10× EC_{50} from Figure 1) or inactive Z isomer during one of three 12 h periods: 5 to 17 hpi (green), 17 to 29 hpi (cyan), or 29 to 41 hpi (purple). Additional Jumonji inhibitors (GSK-J4, ML324, and SD-70) were only tested during the 29 to 41 hpi treatment period at 1×, 5×, or 10× EC_{50}. After the 12 h incubation, parasites were extensively washed to remove drug and returned to the incubator to continue growth. (B−D) Progression through and completion of (reinvasion) the IDC was measured at 50 hpi by flow cytometry as described in the Materials and Methods. (B) Newly invaded rings and (C) remaining trophozoite and (D) schizont parasites that failed to complete the IDC are presented as the fold change relative to vehicle-treated parasites. (E) At the end of each treatment period, a 1:40 dilution of washed parasites was transferred into fresh RBCs and media and cultured for two additional life cycles. Surviving parasites were measured on day 5 by flow cytometry, and data are presented as the fold change relative to vehicle-treated parasites. Data represent the mean ± SEM of 3−6 independent experiments. p values are calculated using a t test between vehicle- and inhibitor-treated samples. ns, nonsignificant; *, $p < 0.05$; **, $p < 0.01$; ***, $p < 0.001$.

and into the next cycle (Figures 2C,D and S2C,D). After 24 h, cultures treated with vehicle or the inactive isomer Z showed enrichment in newly invaded rings and consequently increased parasitemia from 1% to ∼5% (Figures 2C and S2C). Trophozoite cultures treated for 24 h with Jumonji inhibitors showed slight decreases in the number of newly invaded rings,

https://dx.doi.org/10.1021/acsinfecdis.9b00455
ACS Infect. Dis. 2020, 6, 1058−1075

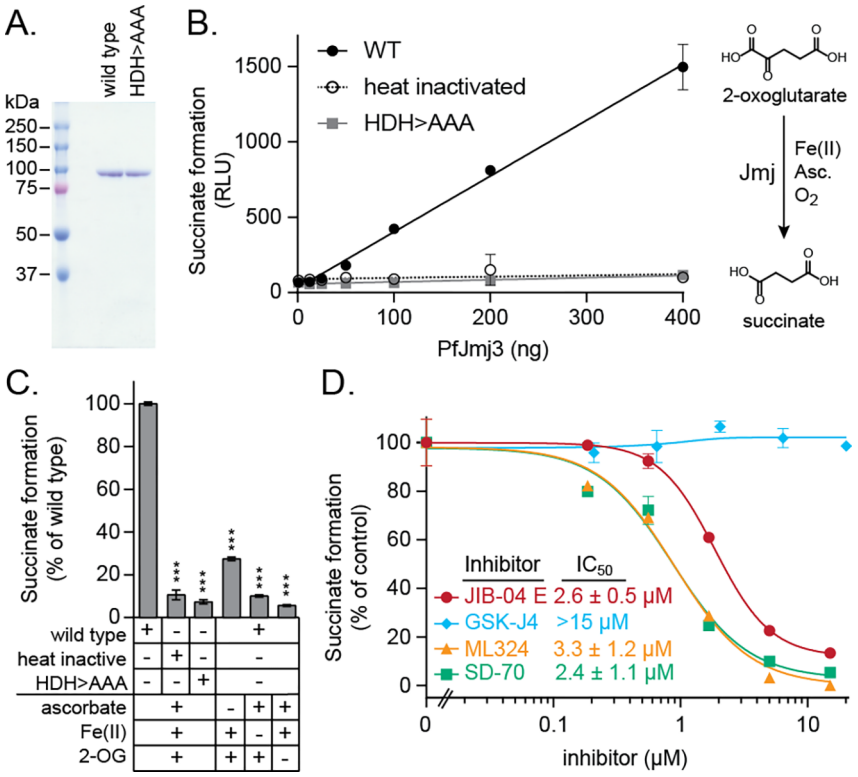

Figure 4. Jumonji inhibitors block the enzymatic activity of recombinant PfJmj3. (A) Purity of wild-type and catalytically dead (HDH > AAA) recombinant PfJmj3 as assessed by Coomassie staining. (B) Representative concentration curves of PfJmj3 enzymatic activity. Succinate formation is measured indirectly through a luciferase-coupled reaction (relative luciferase units (RLUs)). Wild-type PfJmj3, but not heat inactivated wild-type or the catalytically dead HDH > AAA mutant, converts 2-OG to succinate in the presence of Fe(II), ascorbate, and O_2. Data are presented as the mean ± SD of two technical replicates from 1 of 3 independent experiments. (C) Succinate formation by PfJmj3 is dependent upon ascorbate, Fe(II), and 2-OG. Data are presented as a percent of wild-type and represent the mean ± SEM of 3−9 independent experiments. p values are calculated using a t test between vehicle- and inhibitor-treated samples. ns, nonsignificant; *, $p < 0.05$; **, $p < 0.01$; ***, $p < 0.001$. (D) Jumonji inhibitors block the formation of succinate by PfJmj3 in a dose-dependent manner under assay conditions. Data are presented as a percent of the vehicle control and represent the mean ± SD of two technical replicates from 1 of 4−5 independent experiments. IC_{50} concentrations (μM) are the mean ± SEM of the fitted inhibition curves ([inhibitor] vs response − variable slope (four parameters)) from 4 to 5 independent experiments using GraphPad Prism v8.

leading to decreased parasitemia (Figures 2C and S2C). After 48 h, the majority of parasites in control cultures progressed back to trophozoites. In cultures treated with Jumonji inhibitors, we observed significant decreases in trophozoites and those few parasites that have entered schizogony (Figures 2D and S2D). Parasites treated with GSK-J4, ML324, and SD-70 and to a lesser extent JIB-04 E showed increased numbers of the remaining rings (Figures 2D and S2D). These results suggest that a long exposure to Jumonji inhibitors delays progression through the IDC.

Transient Exposure to Jumonji Inhibitors Affects All Stages of the IDC. To test the effects of transient drug exposure throughout the IDC, we treated tightly synchronized 3D7 parasites with increasing concentrations of JIB-04 E for 12 h at defined time periods post-infection (Figure 3A). The 12 h drug exposure was carried out during ring (5−17 hpi), trophozoite (17−29 hpi), or schizont stages (29−41 hpi). After the transient treatment, infected RBCs were washed to remove JIB-04 and reseeded with fresh media to evaluate the ability of the parasite to proliferate post-drug exposure. We then measured parasite reinvasion at ∼50 hpi by flow cytometry. About 80% of infected RBCs from vehicle-treated cultures contained newly invaded rings constituting the bulk parasitemia, with very few trophozoites and schizonts remaining from the previous cycle (Figure S3A). Transient exposure of rings, trophozoites, or schizonts to the lowest concentration of JIB-04 E (1× EC_{50}) decreased the number of newly invaded rings by 40%, 50%, and 75%, respectively, relative to vehicle-treated parasites (Figure 3B, red bars). Higher doses (5× and 10× EC_{50} concentrations) of JIB-04 E produce an even more severe phenotype (Figure 3B). The decrease in newly invaded rings at 50 hpi corresponds to an increase in remaining trophozoites that failed to complete the IDC (Figure 3C). In line with the data from Figure 2, exposure of rings, trophozoites, or schizonts to the lowest concentration of JIB-04 E caused a slight but significant increase in the remaining schizonts (Figure 3D). However, with increasing concentrations of JIB-04 E, we observed an accumulation of trophozoites (Figure 3C) and fewer schizonts (Figures 3D and S3A). Surprisingly, these parasites maintain a mitochondrial membrane potential indicating they are still alive at the 50 hpi time point (Figure S3B). Transient exposure to the inactive Z isomer at the same concentrations as E showed minor effects on progression, consistent with its lower potency (see Figure 1A).

To determine if parasites are merely delayed in development compared to controls or actually arrested, we monitored the progression of late stage parasites (29−41 hpi time period) treated with the lowest concentration of inhibitor at 50, 53, 56, 60, and 72 hpi (Figure S3C). The numbers of remaining

https://dx.doi.org/10.1021/acsinfecdis.9b00455
ACS Infect. Dis. 2020, 6, 1058−1075

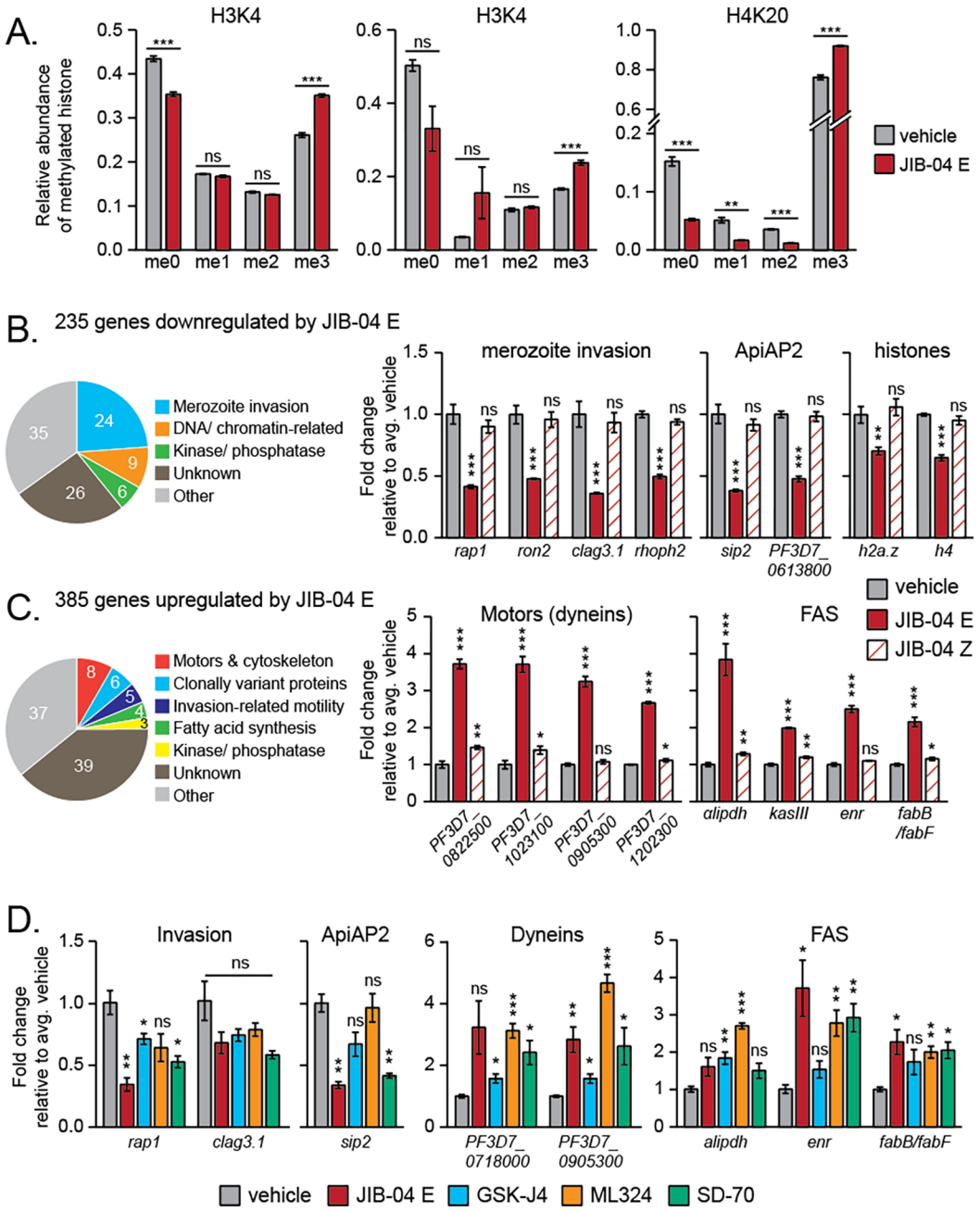

Figure 5. JIB-04 E increases global trimethylated histone marks and deregulates transcription in the IDC. (A) Relative abundance of histone methylation on H3K4, H3K9, and H4K20 in 29 hpi parasites treated with vehicle or 4.5 μM JIB-04 E for 6 h. Bar graphs represent the mean ± SEM of three biological replicates. p values are calculated using a t test between vehicle- and inhibitor-treated samples. (B, C) Functional categorization of genes whose expression levels are deregulated by JIB-04 E on the basis of gene ontology analysis and literature review. See also Table S3. Examples of genes (B) down- or (C) upregulated in 29 hpi parasites treated for 6 h with 4.5 μM JIB-04 E compared to the vehicle and Z isomer. Data are presented as the fold change relative to vehicle-treated controls (mean ± SEM of four replicates). p values are calculated using a t test between vehicle- and inhibitor-treated samples. (D) qRT-PCR analysis of select genes from 29 hpi parasites treated with vehicle or 3× EC_{50} concentrations of Jumonji inhibitors for 6 h as above. Data are presented as the mean ± SEM of the fold change relative to vehicle-treated controls from three biological replicates. p values are calculated using a t test between vehicle- and inhibitor-treated samples. n.s., nonsignificant; *, $p < 0.05$; **, $p < 0.01$; ***, $p < 0.001$.

trophozoites and schizonts at 53, 56, and 60 hpi increased compared to 50 hpi. However, even at the latest time points, we do not observe additional newly invaded rings in the JIB-04 E-treated cultures, suggesting a block at the schizont to ring transition. By 72 hpi, this increase in remaining late stages has disappeared without a corresponding increase in newly invaded rings. Indeed, these parasites failed to complete the IDC and have died on the basis of the loss of membrane potential (Figure S3D). Again, we see no difference between the inactive Z isomer and the vehicle (Figure S3C).

We next tested the effects of transient exposure of late stage parasites to the other Jumonji inhibitors (29–41 hpi only). Treatment with GSK-J4 (cyan bars) and SD-70 (green bars) significantly reduced the number of parasites completing the IDC at all concentrations tested (Figure 3B). Interestingly, treatment with the lowest concentration of ML324 (orange)

https://dx.doi.org/10.1021/acsinfecdis.9b00455
ACS Infect. Dis. 2020, 6, 1058–1075

had minor effects on the number of newly invaded rings, whereas the higher concentrations showed similar reductions in parasite numbers as the other Jumonji inhibitors. Similar to JIB-04 E, the decrease in newly invaded rings upon exposure to the other inhibitors corresponds to an increase in the remaining late stages. The lowest doses cause an accumulation of schizonts (Figure 3D), while the higher doses have earlier effects resulting in trophozoite accumulation (Figure 3C). We further analyzed the cell cycle progression of these remaining late stage parasites by a more in depth analysis of the DNA content (Figure S3E). Increasing concentrations of Jumonji inhibitors result in a greater number of parasites with 1N−3N nuclei and fewer segmented schizonts with >3N nuclei relative to vehicle controls. Together, these data suggest that transient exposure of late stage parasites to Jumonji inhibitors results in a cell cycle arrest phenotype.

Finally, we sought to determine if transient 12 h JIB-04 treatment at different stages had long-term effects on parasite proliferation and if the effects were distinct depending on the stage of parasites during treatment. For this purpose, after each treatment period, a 1:40 dilution of the washed parasites was seeded into fresh media and RBCs, and cultures were allowed to recover for 2.5 IDCs. On day 5 after seeding (scheme shown in Figure 3A), we measured total parasitemia by flow cytometry. Exposure to 1× EC_{50} concentrations of JIB-04 E for only 12 h had no significant effect on the recovery of parasites treated during the ring (5−17 hpi) or trophozoite (17−29 hpi) periods (Figure 3E, first red bar). However, parasitemia was inhibited by about 75% in cultures exposed to the transient drug treatment during the schizont stage (29−41 hpi) at the low dose of JIB-04 E relative to vehicle. At higher doses, transient exposure to JIB-04 E had long-term effects on all parasite cultures, regardless of the stage during treatment. Exposed rings were significantly less affected, and schizonts were most severely affected, with parasitemia at the low end of detection for the latter (Figure 3E, second and third red bars). As before, the inactive Z isomer had little effect on parasite recovery. These results show that a 12 h transient exposure to Jumonji inhibitors has both immediate and long-term effects on *P. falciparum* asexual development in RBCs with late stage parasites having greater sensitivity.

Jumonji Inhibitors Block PfJmj3 Catalysis. To determine if our mammalian Jumonji inhibitors directly target the Plasmodium enzymes, we overexpressed and purified recombinant PfJmj3 as described in the Materials and Methods. As a control, we also purified a catalytically dead mutant version of PfJmj3 in which the iron binding residues (H166, D168, H342) were mutated to alanine (referred to as HDH > AAA). Both proteins were purified to homogeneity as confirmed by Coomassie staining (Figure 4A). Since the endogenous substrate for PfJmj3 is unknown, we measured the conversion of the 2-OG cosubstrate to succinate, the first step in Jumonji catalysis (Figure 4B). This step of the reaction is amenable to small molecule inhibition.[40] Increasing concentrations of wild-type recombinant PfJmj3 resulted in increasing concentrations of succinate formation (Figure 4B). This activity is dependent on the cofactors, ascorbate and Fe(II), as well as the cosubstrate, 2-OG, consistent with the action of the Jumonji family of enzymes (Figures 4C and S4A,B). In contrast to the wild-type protein, neither heat inactivated PfJmj3 nor the HDH > AAA mutant showed activity. We next tested PfJmj3 enzymatic activity in the presence of JIB-04 and other mammalian Jumonji inhibitors. Increasing concentrations of active JIB-04 E, but not the inactive Z form, inhibited PfJmj3 activity with an IC_{50} of 2.6 μM under the assay conditions, i.e., micromolar enzyme (Figure S4C). ML324 and SD-70 also inhibited PfJmj3 activity with similar IC_{50} concentrations, 3.3 and 2.4 μM, respectively (Figure 4D). Interestingly, GSK-J4 had no effect on PfJmj3 activity, suggesting this Jumonji inhibitor does not exert its antimalarial effects through PfJmj3 inhibition. These data indicate that JIB-04, ML324, and SD-70 have the capability of directly blocking the catalysis of 2-OG to succinate by PfJmj3, the first step in all Jumonji reactions independent of the substrate.

JIB-04 E Increases Global Levels of Trimethylated Histones. Of the two families of histone demethylases, only Jumonji proteins are enzymatically capable of catalyzing the demethylation of trimethylated lysine residues in histones.[12,21] To investigate if Jumonji inhibitors target histone methylation patterns in *P. falciparum* similar to their action in mammalian cells, we performed high-resolution nanoLC-MS/MS to quantify changes in histone post-translational modifications. Histones were purified from parasites treated acutely with 4.5 μM JIB-04 E (3× EC_{50}) or the vehicle for 6 h starting at 29 hpi since these parasites showed higher sensitivity (see Figure 3 in which parasites were treated with 5× and 10× EC_{50} concentrations for 12 h). Consistent with the action of Jumonji inhibitors, we observed significant increases in the trimethylation of H3K4 (a histone mark associated with gene activation in *P. falciparum*[5]). Similarly, we observed increased H3K9me3 (a heterochromatin mark in *P. falciparum*) and H4K20me3 (proposed to mark active/poised chromatin) levels after exposure to JIB-04 E (Figure 5A).[5,41−43] There were significant decreases in the unmethylated residues for all three measured marks and lower mono- and dimethylated forms for H4K20 (Figure 5A). Levels of trimethyl H3K36, the reported *var*-specific silencing mark, were below the levels of detection in both inhibitor-treated and control samples.[15,44] Together, these results suggest specific inhibition of Jumonji trimethyl-demethylase enzyme activities.

We also examined histone methylation in parasites treated with the more selective mammalian Jumonji inhibitor, GSK-J4, which showed activity against asexual stage parasites in culture (see Figure 1A) but not against recombinant PfJmj3 (see Figure 4D). GSK-J4-treated (9 μM, 3× EC_{50}) parasites showed higher trimethylation of H3K4 and H4K20 similar to JIB-04-treated parasites but no changes in H3K9me3 (Figure S5A). In contrast to methylation, we observed no changes in the levels of acetylated histones, including the transcriptionally coupled H3K9ac, H3K14ac, and H4K8ac marks in parasites treated with either Jumonji inhibitor (Figure S5A,B).[17,43,45,46] These results show that the exposure of malaria parasites to Jumonji inhibitors disrupts histone trimethylation patterns (more broadly for JIB-04 than for GSK-J4), likely causing deregulation of transcriptional cascades.

Jumonji Inhibitors Disrupt Normal Gene Activation and Silencing in *P. falciparum*. Given the changes in histone methylation observed above and the role of histone methylation in transcriptional regulation, we next determined the effect of Jumonji inhibitors on the *P. falciparum* transcriptome. We first performed global transcriptional profiling on 29 hpi 3D7 late stage parasites treated with either vehicle, 4.5 μM JIB-04 E or 4.5 μM inactive Z isomer, for just 6 h as above to avoid secondary effects on parasite viability. RNA was isolated from four replicates and prepared for sequencing using the Illumina-based platform. We obtained expression data for

https://dx.doi.org/10.1021/acsinfecdis.9b00455
ACS Infect. Dis. 2020, 6, 1058−1075

over 5300 genes, which mapped to 94% of the *P. falciparum* genome. Unsupervised hierarchical clustering segregated vehicle- and inactive Z-treated samples away from JIB-04 E-treated samples (Figure S5C), indicating reproducible transcriptional changes. Differential expression analysis was performed with a cutoff value of 1.5-fold change and FDR of 0.05 (Figure S5D). A comparison of differentially expressed genes between JIB-04 E and control cultures resulted in 235 down- and 385 upregulated genes (Figure 5B,C and Table S3), representing ∼4.5% and 7.5% of the *P. falciparum* genome, respectively. Unlike HDAC inhibitors, we do not see a global disruption of the transcriptome.[47,48]

The majority of gene functional groups that have a defined temporal expression throughout the IDC were not affected by JIB-04 E (Table S4 and Figure S5E).[49] The one exception was downregulation of merozoite invasion genes (Fisher exact test, probability = 1×10^{-9}, Figure 5B and Table S4). This was confirmed by Gene Ontology (GO) and Malaria Parasite Metabolic Pathways (MPMP) analysis of the 235 genes downregulated by JIB-04 E, which indicated that 24% are related to merozoite invasion (Figure 5B and Tables S3, "GO terms-Down" tab, and S4, "Statistical analysis" tab). The expression of invasion-related gene families, including *clag*, *rap*, and *ron*, are significantly decreased by JIB-04 E but not the inactive Z isomer (Figures 5B and S5F and Table S4). A similar pattern was seen with the components of the glideosome (*gap* and *gapm* gene families) (Figure S5F and Table S4).

In addition to invasion genes, other gene categories identified by gene ontology downregulated by JIB-04 included DNA/chromatin related genes (9% of the 235 genes) and kinase/phosphatase genes (6%) (Figure 5B). For example, several histones, and histone- and DNA-binding genes were significantly inhibited in JIB-04 E-treated parasites including AP2 transcription factors (*sip2*, *ap2-o2*, *PF3D7_0613800*, and *PF3D7_0802100*). Together, these data indicate that JIB-04 E treatment downregulates discrete developmental pathways in *P. falciparum*. In addition, JIB-04 also downregulates genes of unknown function and genes that do not fall into major biological categories, which together represent undefined drug targets.

The majority of the 385 genes upregulated by JIB-04 E either were of unknown function (39%) or did not fall into functional categories (37%) as shown in Figure 5C. The remaining 24% upregulated genes were divided among gene families related to motors and cytoskeleton, clonally variant proteins, invasion-related motility, fatty acid synthesis, and kinases/phosphatases (Table S3, "GO terms-Up" tab). For example, JIB-04 E treatment caused an increase in several dynein, kinesin, and myosin genes (Figure 5C and Table S3). JIB-04 E also upregulated variant surface protein genes known to be controlled epigenetically including rifins (Figure S5G and Table S3).[5,15,41] Among the upregulated fatty acid synthesis genes were *fab b/f*, *kasIII*, and *enr* and genes encoding enzymes acting on pyruvate upstream of acetyl CoA production (Figure 5C and Table S3).

To validate the generality of the above transcriptional changes induced by JIB-04 E, we performed qRT-PCR on a subset of genes deregulated by JIB-04 E on parasites treated with the other Jumonji inhibitors (Figures 5D and S5H,I). In agreement with the RNA-seq data, GSK-J4, ML324, and SD-70 showed a similar trend to JIB-04 E in reducing the expression of *rap1*, *clag3.1* (Figure 5D), *ron2*, and *gap50* (Figure S5H) from the various invasion-related gene families. Various Jumonji inhibitors also downregulated the expression of DNA/chromatin-related genes such as the AP2 transcription factor *sip2* (Figure 5D) and histones (Figure S5H). Similar to JIB-04 E, several Jumonji inhibitors activated the expression of genes involved in motor activity and invasion (dynein heavy chains, *ctrp*, *tramp*, and *plasmepsin X*) and fatty acid synthesis (*alipdh*, *enr*, and *fab b/f*) (Figures 5D and S5I). Interestingly, we observed weaker activation of some genes by GSK-J4 compared to the other Jumonji inhibitors. Thus, regulation of these gene sets generally parallel the antimalarial activity of the inhibitors, their effects on parasite progression through the IDC, their effects on histone trimethylation, and their inhibition of PfJmj3 activity *in vitro*.

JIB-04 E Modulated Genes Are Targets of Specific Transcriptional Regulators. Regulation of invasion genes during the IDC is mediated in part through binding of the AP2 transcription factor AP2-I to the "rhoptry motif", found upstream of invasion-related genes including *rap* and *rhoph* gene families.[19,50] PfAP2-I activates transcription of genes in concert with two associated chromatin reader proteins, bromodomain protein 1 (PfBDP1) and chromodomain protein 1 (PfCHD1).[50] PfBDP1, which binds H3K9ac *in vitro*, was also found enriched upstream of micronemal genes, likely regulating these genes in complex with another AP2 transcription factor.[50,51] We find that 36% of genes bound by PfAP2-I (Fisher *t* test, $p = 2.2 \times 10^{-6}$) and 22% of PfBDP1 target genes (Fisher *t* test, $p = 1.7 \times 10^{-13}$) are downregulated by JIB-04 E (Figure 6A and Table S3, "RNA-seq_Down" tab).[50,51] Of the 89 genes that are coregulated by both PfAP2-I and PfBDP1, JIB-04 E inhibits 54 of them (i.e., 60% of genes in this entire set), including invasion-related gene families (*rap*, *rhoph*, *gap*, *gapm*) and several kinases, two of which (PKAr and PKAc) are involved in parasite egress.[52,53] PfBDP1 and PfAP2-I also cobind the promoters of a number of nucleosome and chromatin-binding genes, including histones and seven AP2 genes.[50] Of these, JIB-04 E downregulates 3 core histones, 2 variant histones, *set10*, *chd1*, and the AP2 transcription factor, *sip2* (Table S3). An additional 63 genes targeted by PfBDP1, but not PfAP2-I, were also downregulated by JIB-04 E (Figure S6A). These include additional rhoptry genes (*ron*, *msp*) as well as an AP2 transcription factor (*PF3D7_0613800*). Furthermore, an additional 20 genes bound by PfAP2-I, but not PfBDP1, were also significantly affected by JIB-04 E treatment (Table S3). These results suggest that JIB-04 E prevents activation of invasion-related genes as well as DNA- and chromatin-binding genes by interfering, either directly or indirectly, with transcriptional activating complexes containing PfBDP1 and/or PfAP2-I. Indeed, JIB-04 E treatment strongly mimics the transcriptional changes observed in the *PfBDP1* knockdown and downregulates 34 out of the 47 genes decreased upon BDP1 loss of function ($p = 2.2 \times 10^{-16}$; Table S3).[51]

We noted that many of the genes upregulated by JIB-04 E and not expressed in our control parasites (<5 RPKM) have predicted roles in the other stages of the *P. falciparum* life cycle. Using a manually curated data set from a literature search, we analyzed this gene set against genes known to be specifically expressed in gametocyte and ookinete stages (Tables S3, "RNA-seq_Up" tab, and S4, "GC-ookinete list" tab).[18,54] We find that 115 of the 385 genes upregulated by JIB-04 E are expressed >5-fold higher in gametocytes or ookinetes compared to asexual parasites (Fisher *t* test, $p = 2.2$

https://dx.doi.org/10.1021/acsinfecdis.9b00455
ACS Infect. Dis. 2020, 6, 1058−1075

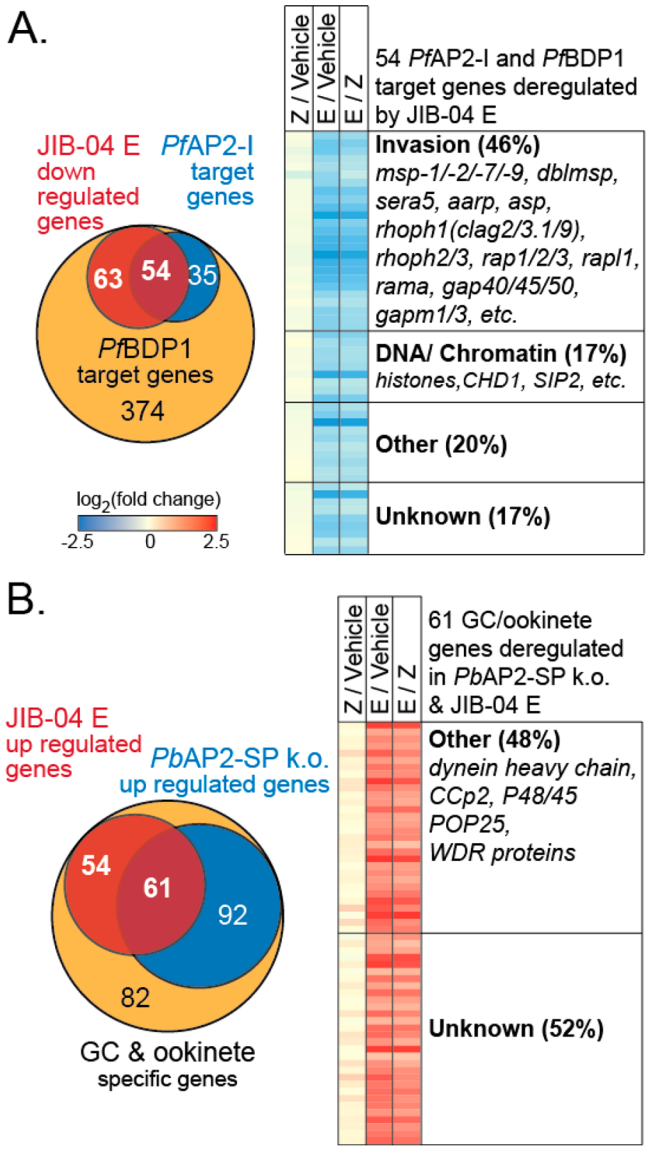

Figure 6. JIB-04 E deregulates genes that overlap known invasion and gametocyte transcription- and chromatin-binding factor targets. (A) Venn diagrams of genes downregulated by JIB-04 E (red) that overlap with PfBDP-1 (orange) and PfAP2-I (blue) target genes. Heat map showing the differential expression between JIB-04 E and the controls of the 54 genes common to all three groups. See also Table S3 and S4. (B) Venn diagrams showing the overlap of genes upregulated by JIB-04 E (red) with gametocyte and ookinete-specific genes (orange) and genes upregulated in *P. berghei* schizonts lacking PbAP2-SP (blue). Heat map showing the differential expression between JIB-04 E and the controls of the 61 genes common to all three groups. See also Tables S3 and S4.

$\times 10^{-16}$) (Figure 6B and Tables S3 and S4). These sexual-stage genes are expressed at relatively low levels in the control cultures (<5 RPKM), and JIB-04 E treatment activates them (Figures 6B and S6B). We also found significant overlap (162 of 385) with genes upregulated in the knockout of PbAP2-SP (Fisher *t* test, $p = 2.2 \times 10^{-16}$), a transcription factor essential for the development of infectious ookinetes in *P. berghei* (Tables S3 and S4).[55] 61 of these genes were also highly expressed in sexual stages and overlap among the three data sets (Figure 6B). These include gametocyte-specific genes, such as 6-cysteine protein P48/45 and several WD40 repeat (WDR) proteins, as well as ookinete-specific genes, such as PSOP25 (Figure S6B). Parasites treated with the other Jumonji inhibitors also show abnormal activation of the gametocyte-specific gene, *pf11-1*, and the ookinete-specific AP2 transcription factor, *ap2-o3* (Figure S6C). These results suggest that JIB-04 E is activating genes normally silenced during the *P. falciparum* IDC possibly through a transcription factor functionally akin to *P. berghei*'s AP2-SP. Overall, Jumonji inhibitors thus disrupt only discrete programs of the normal *P. falciparum* transcriptome including blocking invasion related gene activation and aberrantly turning on the expression of genes specific to sexual parasite forms, without globally altering gene expression patterns.

DISCUSSION

In this study, we took a pharmacological and biochemical approach to probe the role of Jumonji enzymes in the malaria parasite, *Plasmodium falciparum*. We show that several small molecule inhibitors of mammalian Jumonji histone lysine demethylases disrupt growth of asexual and sexual stage parasites. In fact, gametocyte development and the formation of gametes are highly sensitive to JIB-04 E with EC_{50} concentrations in the nanomolar range (0.01−0.12 μM). This hypersensitivity toward sexual stages compared to asexual stages could result from differences in the expression levels and/or essentiality of the PfJmj enzymes during gametocytogenesis and gamete formation, leading to transcriptional disruption of gene programs involved in sexual development. Alternatively, variations in iron, 2-OG, oxygen, ascorbic acid, and even succinate levels between the stages could contribute to this difference in potency. Previous studies have demonstrated that inhibitors of histone lysine methyltransferases (KMTs), the writers of methylation, block asexual stage growth, gametocyte development, and gamete formation.[56−58] Male gametes were about 10-fold more susceptible to inhibition of the G9a KMT than female gametes.[57] We observe a similar shift in EC_{50} with the Jumonji inhibitor JIB-04 E (0.01 vs 0.08 μM for male vs female gamete formation), highlighting an essential role of histone methylation homeostasis for transmission to the anopheline vector.

Studies targeting histone acetyl transferase, histone deacetylase, and KMT enzymes have implicated histone modifications in regulating the complex life cycle of the malaria parasite, but the role of KDMs, the erasers of methylation, remained largely unstudied.[47,48,56−63] Jiang et al. have shown that neither PfJmjC1 nor PfJmjC2 are essential for *in vitro* asexual development in the erythrocyte.[15] Interestingly, neither the *PfJmjC1* nor *PfJmjC2* knockout mimicked the *var* gene deregulation phenotype of the *SETvs* KMT knockout, suggesting redundancy or compensation of KDM activity by another PfJmj enzyme.[15] In a recent transposon mutagenesis screen, *PfJmj3* mutant parasites while viable did exhibit a low mutagenesis fitness score (−2.57), indicating a fitness cost for *in vitro* asexual growth due to disruption of the gene.[20] Unlike the above studies, our approach using small molecule inhibitors potentially targets all three *P. falciparum* Jumonji enzymes. Our *in vitro* biochemical studies show that Jumonji inhibitors inhibit the enzymatic activity of recombinant PfJmj3, while our molecular and mass spectrometry data suggest that inhibitors reduce Jumonji histone demethylase activity on multiple trimethylated histone marks. Thus, their action on the parasite is at least partly on target and may represent the cumulative effect on multiple Jumonji enzymes. Of interest is

https://dx.doi.org/10.1021/acsinfecdis.9b00455
ACS Infect. Dis. 2020, 6, 1058−1075

the difference between GSK-J4 and the other inhibitors evaluated here. GSK-J4 does not inhibit the enzymatic activity of PfJmj3 *in vitro* nor does it increase the levels of H3K9me3 in the parasite, in contrast with JIB-04. It does, however, increase other trimethyl histone marks including H3K4me3 and H4K20me3, suggesting a different target specificity from JIB-04, ML324, and SD-70.

Trimethylation of multiple lysine residues on H3 and H4 has been well documented in *P. falciparum*. H3K4me3 is a euchromatic mark highly enriched in late stage asexual parasites.[5,17,45,64−66] Although the exact role of this mark in *P. falciparum* is still unclear, it is likely associated with transcriptional activity.[67] H3K9me3 is a repressive mark specifically localized to telomeres and subtelomeric repeats and has a well characterized role in regulating clonally variant gene expression in *P. falciparum*.[5,11,42,68] The H4K20me3 mark has been reported in *P. falciparum* with global levels peaking in schizonts, but its function in the parasite is still unknown.[5,43,45,66] Our studies provide evidence that mammalian Jumonji inhibitors block the histone demethylase activity of at least one of the three *P. falciparum* Jumonji enzymes *in vivo*, resulting in increased levels of histone methylation, and/or directly block PfJmj3 catalysis *in vitro*. Given the specificity achieved among the mammalian Jumonji KDMs within the active site pocket, it is plausible that inhibitors specific to the *P. falciparum* Jumonji's might be designed without toxicity to healthy cells. Furthermore, since in the cancer setting JIB-04 and other inhibitors have shown robust selectivity for the disease state, not affecting normal cells, there is potential for parasite-targeting analogs to have a strong therapeutic window against the most sensitive sexual stages.

In line with the disruption of trimethyl histone marks, JIB-04 E altered the expression of 620 genes in parasites (∼12% of the *P. falciparum* genome). We observed up- and downregulation of gene expression, leading to misregulation of specific transcriptional programs, in agreement with the discrete effects of Jumonji inhibitors also seen in cancer cells and tumors.[32,69] These transcriptional changes were replicated with other Jumonji inhibitors, indicating an overlapping mechanism of action and common gene targets. Our results are in contrast to the effects of HDAC inhibitors such as apicidin and trichostatin A, which caused more global changes of the IDC transcriptome, affecting from ∼30% up to 60% of the *P. falciparum* genome.[47,48]

The majority of genes downregulated by Jumonji inhibition either were annotated as unknown function or did not fall into any known GO group, representing yet undefined targets of Jumonji inhibition. Of interest, a subset of downregulated genes were enriched in invasion-related genes and a surprising number coincided with loci regulated in *P. falciparum* by the chromatin reader PfBDP1, the PfAP2-I transcription factor, or both. PfBDP1 and PfAP2-I have been directly implicated as master regulators of invasion gene programs in recent genetic studies.[50,51] The conditional *PfBDP1* knockdown blocks parasite invasion and growth.[51] PfBDP1 has not yet been pharmacologically targeted, and targeting transcription factors such as PfAP2-I is notoriously challenging. Jumonji inhibitors partly disrupt PfBDP1 and/or PfAP2-I transcriptional programs and may thus block parasite invasive capacity through modulation of histone methylation at these loci. Indeed, JIB-04 treatment mimics gene downregulation in the *PfBDP1* knockdown and may thus be a surrogate inhibitor for this chromatin interacting protein.[51]

Whether the Jumonji inhibitors evaluated here are exerting their antimalarial effects also by affecting nontranscriptional pathways remains an open question. A growing number of nonhistone targets of Jumonji enzymes, including transcription factors, enzymes, and tRNA, have been identified in other systems.[70] This may also be the case in *Plasmodium falciparum*. It is feasible that inhibition of PfJmjC2, for example, may affect the parasite's wybutasine pathway, disrupting translational control since PfJmjC2 closely resembles the mammalian Jumonji enzyme TYW5.[71] On the basis of sequence homology, PfJmj3 aligns with Jumonji protein hydroxylases, suggesting a potential role for protein hydroxylation in the malaria parasite in addition to histone demethylation. Recent studies have shown that Jumonji hydroxylases have roles in protein translation, cell division, and development.[72−74] For example, human JMJD7 was reported to hydroxylate lysine residues on developmentally regulated GTP-binding proteins 1 and 2 (DRG1/2), increasing the complex's affinity for RNA, whereas human JMJD5 can modify arginine residues on the chromosome condensation domain containing protein 1 (RCCD1) and ribosomal protein S6 (RPS6).[72,73] Thus, future work will need to identify the histone, nonhistone protein, and nonprotein substrate(s) of all three *P. falciparum* Jumonji enzymes and establish their functional significance.[40] At present, our studies provide direct evidence that mammalian Jumonji inhibitors block malaria Jumonji enzyme activity *in vitro*, increase histone trimethylation in the parasite, alter discrete transcriptional programs, and disrupt parasite development. These findings suggest that the aggregate activities of the *P. falciparum* Jumonji enzymes are likely essential during the parasite's life cycle.

■ CONCLUSION

Here, we use a pharmacological and biochemical approach to probe the role of Jumonji enzymes in the malaria parasite. Jumonji enzymes are transcriptional regulators that in other known systems erase methylation from histones affecting gene expression. We show that in *Plasmodium falciparum* inhibitors of mammalian Jumonji enzymes trigger the accumulation of histone methylation, deregulate gene expression programs, halt parasite development, and lead to parasite death. *In vitro*, the inhibitors block the catalytic activity of a purified malaria Jumonji enzyme. Together, these findings suggest that the aggregate activity of the malaria Jumonji enzymes is likely essential during the parasite's life cycle.

■ MATERIALS AND METHODS

Parasites and Culturing. For asexual stage experiments, 3D7 and Dd2 parasites were cultured at 2% to 4% hematocrit in male O+ red blood cells (Valley Biomedical, Winchester, VA) in RPMI 1640 media with L-glutamine and 25 mM HEPES (Sigma-Aldrich, St. Louis, MO) supplemented with 5% Albumax I (Gibco, Life Technologies, Carlsbad, CA), 12 μg/mL hypoxanthine (Sigma, St. Louis, MO), and 23 mM sodium bicarbonate.[75] Cultures were maintained in a humidified incubator at 37 °C under a 5% O_2/5% CO_2/90% N_2 gas mixture. When parasites were maintained at a parasitemia greater than 4% for particular experiments, cultures were fed twice daily. Parasite lines were regularly tested for mycoplasma by PCR using the primers Myco Forward 5′-CCGCGGTAATACATAGGTCGC and Myco Reverse 5′-CACCATCTGTCACTCTGTTAACC. Parasitemia was moni-

https://dx.doi.org/10.1021/acsinfecdis.9b00455
ACS Infect. Dis. 2020, 6, 1058−1075

tored by blood smears stained with Giemsa (Sigma-Aldrich) diluted in pH 7.2 buffer (Millipore, Billerica, MA). Images of stained parasites were acquired using an Infinity 1-2CB camera and Analysis software (Lumenera Corp., Ottawa, Canada). 3D7 and Dd2 parasites were a gift from Dr. Margaret Phillips (UT Southwestern).

Gametocyte development assays were performed using the NF54 peg4-tdTomato reporter line[76] with media supplemented with 0.25% AlbuMax II (ThermoFisher, Waltham, MA) and 5% human serum (NY Blood Center, New York, NY). For the dual gamete-formation assays, NF54 parasites (MRA-1000, BEI Resources, Manassas, VA) were cultured in media supplemented with 10% human serum (obtained from Biobancos de Castilla y Leon, Barcelona and Centro de Transfusiones de Madrid and the Red Cross Transfusion Blood Bank in Madrid, Spain).

Chemical Compounds. Chloroquine (Sigma-Aldrich) was dissolved in H_2O, whereas all other drugs were dissolved in DMSO (Sigma-Aldrich). The Jumonji inhibitors used in this study were obtained from Cayman Chemical, Ann Arbor, MI (GSK-J4, GSK-J5, and CPI-455), Selleck Chemicals, Houston, TX (ML324), and Xcess Biosciences, San Deigo, CA (KDM5-C70 and SD-70). JIB-04 E and Z isomers were synthesized as previously described.[23] Compounds freshly dissolved in DMSO were aliquoted to minimize freeze/thaw cycles and stored at −20 °C.

EC_{50} Determination. Compound EC_{50} concentrations were determined using the 3 day SYBR green assay as described in Smilkstein et al. with slight modifications.[30] Parasites were synchronized to ring stages using 5% sorbitol for two cycles prior to the experiment. On day 0, ring stage parasites were seeded into the inner wells of a 96-well black plate with a clear bottom (Costar, Tewksbury, MA) at 0.5% parasitemia and 2% hematocrit. Drug was added such that each well received the same concentration of DMSO (final DMSO concentration <0.5%). Each plate contained vehicle-only and chloroquine (0.25 μM for 3D7 and 5 μM for Dd2) controls. Parasites were incubated at 37 °C in the presence of compounds for 72 h after which thin blood smears were made and plates were frozen at −80 °C. On a subsequent day, plates were thawed at RT and 100 μL of 2× SYBR Green I (Sigma-Aldrich) in lysis buffer (20 mM Tris-HCl, pH 7.5, 5 mM EDTA, 0.008% w/v saponin, and 0.03% v/v Triton X-100) was added to each plate. Plates were then incubated in the dark at RT for 4 h. Fluorescence was measured on a BioTek (Winooski, VT) Synergy H1 Hybrid plate reader using a 485 nm excitation filter and a 535 nm emission filter. EC_{50} values were calculated as a percentage of parasite viability relative to vehicle-only and chloroquine-killed controls. A nonlinear regression curve ([inhibitor] vs response − variable slope (four parameters): $Y = \text{bottom} + (\text{top} - \text{bottom})/(1 + (IC_{50}/X)^{\text{hill slope}})$) was fit to the data using GraphPad Prism version 8. Each plate contained three technical replicates. Mean EC_{50} concentrations and SEM were calculated from at least 3 independent experiments.

Gametocyte Development Assays. Synchronous gametocytes were obtained following a method adapted from Fivelman et al.[77] *P. falciparum* sexual development assays were performed using the NF54 peg4-tdTomato reporter line[76] in 96-well flat bottom plates. Twice synchronized trophozoites were cultured in suspension at 2% parasitemia and 3% hematocrit in flasks. Parasites were allowed to reinvade new red blood cells, and the culture was maintained in the subsequent 48 h cycle at about 8−9% parasitemia and 3% hematocrit (sexual commitment cycle). At the end of the commitment cycle, segmented schizonts were purified using a Percoll-sorbitol gradient and then combined with fresh erythrocytes in complete media at 3% hematocrit and around 10% parasitemia for 3−4 h to allow for reinvasion. When the ring parasitemia reached 3.5%, remaining late stages were removed via a Percoll-sorbitol gradient, and the newly invaded ring parasites were washed three times with incomplete media. On day +1 (first day of gametocyte development), parasitemia and pre-existing gametocytemia were assessed by flow cytometry (Cytek DxP11) on the basis of Hoechst 33342 DNA staining (375 nm laser, 450/50 emission filter) and the tdTomato fluorescent signal (561 nm laser, 590/20 emission filter). Plates were set up with 200 μL of drug media per well containing the compound of interest and 50 mM *N*-acetylglucosamine at 3.5% parasitemia and 1% hematocrit. Parasites were cultured for an additional 6 days to allow for gametocyte development, during which media was not changed. On day +6, the gametocytemia was assessed by flow cytometry using Hoechst 33342 DNA staining and tdTomato fluorescent signal.

Gamete Formation Assays. The dual gamete-formation assay was performed as described in Delves et al.[37] NF54 parasites were cultured in media supplemented with 10% human serum and induced to form gametocytes. On day 14 post-induction, stage V gametocytes were seeded into 384-well plates at 1% gametocytemia and 4% hematocrit and exposed to drug for 48 h. To induce male exflagellation and monitor female gametes, ookinete media containing 100 μM xanthurenic acid (Sigma-Aldrich) and 0.5 μg/mL anti-Pfs25-cy3 antibody (MRA-315, BEI Resources) were added. Exflagellation was monitored by phase contrast on a Nikon Ti-E widefield microscope. Plates were incubated for an additional 24 h, and female gamete formation was evaluated by the expression of Pfs25 on the TRITC channel. Exflagellation centers and female gamete formation were quantified using the Icy Bioimage Analysis Program (http://icy.bioimageanalysis.org/). The inhibition of gamete formation by JIB-04 was calculated relative to positive (40 μM gentian violet, MolPort) and negative (DMSO) controls.

Flow Cytometry. Live infected red blood cells were labeled for 30 min in the dark with final concentrations of dyes at 4 μM Hoechst 33342 (Molecular Probes, Eugene, OR), 100 ng/mL thiazole orange (Sigma-Aldrich), and 25 nM $DiIC_1(5)$ (1,1′,3,3,3′,3′-hexamethylindodicarbocyanine iodide, Molecular Probes). Progression through the asexual IDC was assessed by flow cytometry (5-laser BD FACS Aria Fusion SORP or FACS Aria Fusion; The Moody Foundation Flow Cytometry Facility, UT Southwestern) on the basis of Hoechst 33342 DNA staining (355 nm laser, 450/50 emission filter), thiazole orange RNA staining (488 nm laser, 525/50 emission filter), and $DiIC_1(5)$ mitochondrial potential signal (640 nm laser, 670/30 emission filter). 100 000 single cells were counted per sample, and single events were distinguished from doublets using FSC-H and FSC-W gates. Data was analyzed using FlowJo v10 (FlowJo, LLC, Ashland, OR). Infected RBCs with live parasites were defined as Hoechst/DNA-positive and $DiIC_1(5)$/mitochondrial potential-positive according to Grimberg.[78] Parasite stages were separated using Hoechst/DNA and thiazole orange/RNA signals: ring stage parasites were defined as DNA-positive/RNA-negative; trophozoites and early schizonts were defined as <3N DNA-positive/RNA-positive,

https://dx.doi.org/10.1021/acsinfecdis.9b00455
ACS Infect. Dis. 2020, 6, 1058−1075

and schizonts were defined at >3N DNA-positive/RNA-positive.

Stage of Parasite Arrest. 3D7 parasites were synchronized with 5% sorbitol two cycles prior to the experiment. On day 0, a ring stage culture was set up at 3% parasitemia and 2% hematocrit. Half of the culture was seeded into a 24-well plate, and drug was added to measure the effect of the inhibitors on ring stage parasites. On day 1, late stage parasites from the remainder of the starting culture were refed and seeded into a 24-well plate to measure the effect of inhibitors on late stage parasites. At 0, 24, and 48 h after the addition of drug, thin blood smears were made and an aliquot of each sample was analyzed by flow cytometry as described above.

Washout Experiments. 3D7 parasites were tightly synchronized to a 4 h window using 40/70% Percoll-sorbitol gradients and seeded into multiple 96-well plates at 1% parasitemia and 2% hematocrit. At each time point, one plate was removed from the incubator and drug was added in fresh media in triplicate wells. Parasites were resuspended by pipetting to ensure complete mixing, and a thin blood smear was made. After the 12 h treatment period, thin blood smears were made of sample wells. Media containing drug was removed, and cells were washed 2× with fresh media. Fresh media was added, and cells were thoroughly resuspended by pipetting prior to transferring a 1:40 dilution of culture to a second plate containing fresh complete media and RBCs at 2% hematocrit. Plates were then returned to the incubator. At the defined time points, thin smears were made of sample wells and an aliquot of culture was transferred to a V-bottom 96-well plate for staining followed by flow cytometry as described above.

Plasmid Construction. Codon optimized PfJmj3 was synthesized by GenScript with *Bam*HI and XbaI restriction sites flanking the gene and cloned into the pMAL-cHT expression plasmid[79] kindly provided by Dr. Sean Prigge (Johns Hopkins Bloomberg School of Public Health). Catalytically dead PfJmj3 was generated by site-directed mutagenesis using the following primers: for H342A: KM63_For, 5′ - GCCGTGTGGATGGTTTGCCGAGGTGAAAAGCTTC, and KM64_Rev, 5′ - CGGAGCTGAAGCTTTTCACCTCGGCAAACCATCCAC; for H166A and D168A: KM65_For, 5′ - CCAAACTGAAGACATATCTGGCCCATGCTTACCATGAC, and KM66_Rev, 5′ - GCACATAGATATTGTCATGGTAAGCATGGGCCAGATATGTC. The entire open reading frame for both wild-type and HDH > AAA plasmids was confirmed by DNA sequencing (UTSW McDermott Sequencing Core). Plasmids were then transformed in Rosetta (DE3) *Escherichia coli*-competent cells (Novagen, EMD Biosciences Inc., Madison, WI) for protein expression. For protein purification, a single colony was grown in Luria Broth (Research Product International, Mt. Prospect, IL) containing 100 μg/mL ampicillin and 35 μg/mL chloramphenicol.

Protein Purification. Recombinant MBP-PfJmj3 overexpression was induced with 1 mM IPTG at 18 °C overnight. A cell pellet from 8 L of wild-type was resuspended in 120 mL of buffer A (50 mM HEPES, pH 7.5) with 150 mM NaCl containing 0.2 mM phenylmethanesulfonyl fluoride and 3 protease inhibitor tablets (Complete Mini; Roche, Mannheim, Germany) using a dounce homogenizer. Cells were incubated with 200 μg/mL lysozyme and 10 μg/mL DNase at 4 °C for 1 h followed by lysis with a tip sonicator (Heat Systems Inc., Farmingdale, NY) and then subjected to 50 000*g* centrifugation at 4 °C for 30 min. The supernatant was loaded on a MBPTrap HP column (GE Healthcare, Uppsala, Sweden). The column was washed with 50 column volumes of buffer A with 150 mM NaCl, and bound protein was eluted with 10 column volumes of buffer A containing 50 mM NaCl and 10 mM maltose. Protein containing fractions were pooled, diluted with buffer A, and loaded onto a HiTrap Q HP column (GE Healthcare). The column was washed with 50 column volumes of buffer A containing 100 mM NaCl followed by 50 column volumes of buffer A with 300 mM NaCl. Bound protein was eluted with 10 column volumes of buffer A containing 600 mM NaCl. The eluted fractions with the desired protein were pooled and diluted with buffer A to a final concentration of 150 mM NaCl with 20% glycerol and stored at −80 °C until use. Protein concentrations were measured using the DC Protein Assay (BioRad, Hercules, CA). The catalytically dead mutant protein was purified as above from 4 L.

Succinate Assay. Succinate production from recombinant MBP-PfJmj3 was measured using the Succinate-Glo JmjC Demethylase/Hydroxylase Assay (Promega, Madison, WI) according to the manufacturer's instructions. Reaction mixtures (25 μL) containing 50 mM HEPES, pH 7.5, 100 μM ascorbic acid, 10 μM $Fe(II)(NH^4)_2(SO^4)_2$, and 10 μM 2-OG, except where noted, were set up in 96-well plates (half area, white, flat bottom, nonbinding; Corning, Kennebunk, ME). The reaction was initiated by the addition of recombinant MBP-PfJmj3 protein (2 μM) and mixed for 2 min using a plate shaker. For inhibitor reactions, the enzyme was preincubated with 20 μM ascorbic acid and 2 μM $Fe(II)(NH^4)_2(SO^4)_2$ for 10 min on ice after which 10 μM 2-OG and inhibitor were added simultaneously. All inhibitors were dissolved in DMSO at concentrations such that a total of 1 μL was added to each reaction. Inhibition curves were performed using 3-fold serial dilutions starting with 15 μM (to 0.18 μM). After incubation for 1 h at room temperature, 25 μL of Succinate Detection Reagent I was added to each well and mixed for 2 min using a plate shaker. Following incubation for 1 h at room temperature, 50 μL of Succinate Detection Reagent II was added to each well and mixed for 30 s. Luminescence was measured after 10 min on a microplate reader (FLUOstar Omega; BMG Labtech, Cary, NC). Independent experiments for each inhibitor were performed with different batches of enzyme: JIB-04 E (n = 5), JIB-04 Z (n = 2), GSK-J4 (n = 4), ML324 (n = 4), and SD-70 (n = 4). Nonlinear regression curves ([inhibitor] vs response − variable slope (four parameters)) were fit using GraphPad Prism version 8.

Mass Spectrometry Analysis for Histone PTMs. 3D7 parasites were tightly synchronized to a 4 h window as above and seeded at 4% parasitemia and 2% hematocrit. Drug was added at 29 hpi. After 6 h, infected RBCs were pelleted and immediately frozen in liquid nitrogen. After thawing, parasites were isolated from RBCs using 0.05% saponin in cold PBS and subsequently washed 3× in cold PBS. Histones were extracted using the EpiQuik Total Histone Extraction kit (Epigentek, Farmingdale, NY) followed by TCA precipitation. A portion of the histone extracts were run on a 15% SDS-PAGE gel and visualized with Quick Coomassie Stain (Protein Ark, Sheffield, United Kingdom) to determine purity and concentration. Histones were prepared for mass spectrometry by chemical derivatization using propionic anhydride and digested to peptides with trypsin, followed by another round of derivatization. Peptides were desalted using C18 stage tips,

https://dx.doi.org/10.1021/acsinfecdis.9b00455
ACS Infect. Dis. 2020, 6, 1058−1075

and about 1−2 μg of peptides were analyzed using an EASY-nLC nanoHPLC (Thermo Scientific, Odense, Denmark) coupled with a Q-Exactive mass spectrometer (Thermo Fisher Scientific, Bremen, Germany). HPLC gradients and mass spectrometry parameters were defined previously.[80] To facilitate MS/MS-based quantification, both data-dependent acquisition and targeted acquisition for isobaric peptides were included. The relative abundances of histone H3 and H4 peptides were calculated using EpiProfile.[81]

RNA Sequencing and Analysis Pipeline. 3D7 parasites were tightly synchronized to a 3 h window using Percoll-sorbitol gradients. Parasites were seeded into 6-well plates at 4% parasitemia and 2% hematocrit. At 29 hpi, drug was added to each well with a final DMSO concentration of 0.04%. Four replicates were performed for each treatment. One set of cultures was harvested immediately corresponding to 0 h of treatment, and the remaining cultures were harvested after a 6 h incubation. Parasite culture was passed through a Plasmodipur filter (EuroProxima, Arnhem, Netherlands) to remove residual white blood cells. Parasite pellets were immediately lysed in Trizol LS Reagent (ThermoFisher Scientific) and subsequently snap frozen in liquid nitrogen. RNA was isolated according to manufacturer's instructions and precipitated in the presence of linear acrylamide (Amresco, Solon, OH). Samples were prepared from 2 μg of RNA using the Illumina (San Diego, CA) Tru-stranded mRNA library kit according to manufacturer's directions. RNA and library quality were validated on an Agilent 2100 Bioanalyzer prior to sequencing on an Illumina NextSeq 500 (McDermott Next Generation Sequencing Core, UT Southwestern) at an average of 37 000 000 reads per sample. Raw reads were processed (McDermott Center Bioinformatics Core, UT Southwestern) and aligned (STAR aligner) to the *P. falciparum* 3D7 transcriptome (PlasmoDB v. 34).[16] Unique transcripts were mapped to an average of 94% of the transcriptome. Expressed genes were defined as genes with an average expression higher than 0.1 RPKM across the four replicates. Differential expression analysis was performed using EdgeR (Bioconductor).[82,83] We selected genes with a >1.5-fold difference between JIB-04 E and either the vehicle or JIB-04 Z treatment groups and a FDR of <0.05 for further analysis. Gene ontology (GO) enrichment analysis was performed at PlasmoDB.org[16] and Malaria Parasite Metabolic Pathways (MPMP), http://mpmp.huji.ac.il/. Heatmaps and Venn diagrams were generated using Morpheus (https://software.broadinstitute.org/morpheus; Broad Institute) and BioVenn,[84] respectively.

qRT-PCR. RNA was purified using a Trizol LS (ThermoFisher Scientific) extraction method. Approximately 2 μg of RNA was treated with DNase I (Roche) prior to reverse transcription using the High Capacity cDNA Reverse Transcription kit (Applied Biosystems, Foster City, CA). Quantitative PCR (qPCR) was performed in triplicate wells using SYBR Green ER qPCR SuperMix (Invitrogen, Carlsbad, CA). qPCR reactions were run on an ABI 7300 Real-Time PCR System and analyzed with QuantStudio Real-Time PCR software (Applied Biosystems). The ΔΔCt method was used to compute relative mRNA expression with serine tRNA ligase (*PF3D7_0717700*) as the reference gene. The list of primers used is in Table S2.

Bioinformatics Analysis. We compared the differentially expressed gene list to various publicly available data sets. We defined PfBDP1 targets (from Table S6 in ref 51) as those genes with peak ChIP enrichment in either trophozoite or schizont stages and PfAP2-I targets (from Table S2 in ref 50) as those genes with trimmed peak ChIP enrichment in schizonts. We compared our list of differentially expressed genes from JIB-04 E-treated and PbAP2-SP knockout parasites[55] using a cutoff of 1.5-fold and FDR < 0.05. *P. falciparum* orthologs of *P. berghei* gene IDs were determined using PlasmoDB.[16] Using PlasmoDB, we searched the RNA-seq transcriptomes of asexual and sexual stages from Lopez-Barragan et al.[18] for genes with >5-fold expression in stage II or V gametocytes or ookinetes compared to trophozoites or schizonts. We stringently defined stage specific genes as those with <5 FPKM in trophozoites and schizonts and >5-fold expression in gametocytes or ookinetes. We further cross-referenced these genes with the male and female gametocyte transcriptomes from Lasonder et al.[54] Venn diagrams were generated using BioVenn,[84] and Fisher *t* test and hypergeometric distribution of overlap was performed using R i386 version 3.5.3.

Data Availability. All RNA-seq data sets have been deposited under the GEO accession number GSE117307.

■ ASSOCIATED CONTENT

Supporting Information

The Supporting Information is available free of charge at https://pubs.acs.org/doi/10.1021/acsinfecdis.9b00455.

Plasmodium falciparum encoding three Jumonji C domain-containing proteins with conserved active site residues; Jumonji inhibitors impairing the development of ring and late stage-treated parasites; short term exposure to JIB-04 E impairing IDC; recombinant PfJmj3 enzymatic activity dependent on Fe(II) and 2-OG concentration; Jumonji inhibitors deregulating the transcription of a subset of genes and not altering the global histone acetylation during IDC; downregulation of PfBDP1 target gene expression and upregulation of gametocyte and ookinete specific genes by Jumonji inhibitors; Table S1, structures of Jumonji histone demethylase inhibitors used in this study; Table S2, list of QRT-PCR primer sequences (PDF)

Table S3, transcriptome analysis and GO terms of genes deregulated by JIB-04 E (XLSX)

Table S4, functional gene groups and statistical analysis related to Figures 5 and 6 (XLSX)

■ AUTHOR INFORMATION

Corresponding Author

Elisabeth D. Martinez − *Department of Pharmacology and Hamon Center for Therapeutic Oncology Research, The University of Texas Southwestern Medical Center, Dallas, Texas 75390, United States;* orcid.org/0000-0003-1131-3689; Email: elisabeth.martinez@utsouthwestern.edu

Authors

Krista A. Matthews − *Department of Pharmacology, The University of Texas Southwestern Medical Center, Dallas, Texas 75390, United States*

Kossi M. Senagbe − *Hamon Center for Therapeutic Oncology Research, The University of Texas Southwestern Medical Center, Dallas, Texas 75390, United States*

Christopher Nötzel − *Department of Microbiology & Immunology and Biochemistry, Cell & Molecular Biology*

Graduate Program, Weill Cornell Medicine, New York, New York 10065, United States

Christopher A. Gonzales − *Hamon Center for Therapeutic Oncology Research, The University of Texas Southwestern Medical Center, Dallas, Texas 75390, United States*

Xinran Tong − *Department of Microbiology & Immunology, Weill Cornell Medicine, New York, New York 10065, United States*

Filipa Rijo-Ferreira − *Department of Neuroscience, The University of Texas Southwestern Medical Center, Dallas, Texas 75390, United States*

Natarajan V. Bhanu − *Epigenetics Program, Department of Biochemistry and Biophysics, Perelman School of Medicine, University of Pennsylvania, Philadelphia, Pennsylvania 19104, United States*

Celia Miguel-Blanco − *Tres Cantos Medicines Development Campus, GlaxoSmithKline, Tres Cantos, Madrid 28760, Spain*

Maria Jose Lafuente-Monasterio − *Tres Cantos Medicines Development Campus, GlaxoSmithKline, Tres Cantos, Madrid 28760, Spain*

Benjamin A. Garcia − *Epigenetics Program, Department of Biochemistry and Biophysics, Perelman School of Medicine, University of Pennsylvania, Philadelphia, Pennsylvania 19104, United States*

Björn F. C. Kafsack − *Department of Microbiology & Immunology and Biochemistry, Cell & Molecular Biology Graduate Program, Weill Cornell Medicine, New York, New York 10065, United States*

Complete contact information is available at: https://pubs.acs.org/10.1021/acsinfecdis.9b00455

Author Contributions

$^{\nabla}$E.D.M.: Lead contact.

Notes

The authors declare no competing financial interest.

■ ACKNOWLEDGMENTS

We are deeply grateful to Dr. Margaret Phillips for invaluable resources and suggestions and Dr. Jacqueline Njoroge for initial observations. We are grateful to Nicholas Loof and the Moody Foundation Flow Cytometry Core for help with establishing the flow cytometry setup and Dr. Arun Radhakrishnan for his assistance in the protein purification of PfJmj3. Thanks to Drs. Tram Anh Tran and Lei Wang for general project support. This work was partly funded by The Welch Foundation (I-1878 to E.D.M.), by the Alfred & Kathryn Gilman Family Giving Fund (to K.A.M. and E.D.M.), by the John P. Perkins, Ph.D. Distinguished Professorship in Biomedical Science Endowment (to E.D.M.), by the NIH (R21AI139408 to E.D.M. and R01AI141965 to B.F.C.K.), by CPRIT (RP160493 to E.D.M.), by Alice Bohmfalk Charitable Trust Research Grant (to B.F.C.K.), and by the Jacques Cohenca Predoctoral Fellowship (to C.N.).

■ ABBREVIATIONS

Pf, *Plasmodium falciparum*; *Pb*, *Plasmodium berghei*; JmjC, Jumonji C; RBC, red blood cell; 2-OG, 2-oxoglutarate; IDC, intraerythrocytic development cycle; KDM, histone lysine demethylase; EC, effective concentration; GC, gametocyte; hpi, hours post-invasion; GO, gene ontology; BDP1, bromodomain protein 1; KMT, histone lysine methyltransferase

■ REFERENCES

(1) WHO (2018) *World malaria report 2018*, WHO, Geneva.

(2) Merrick, C. J., and Duraisingh, M. T. (2010) Epigenetics in Plasmodium: what do we really know? *Eukaryotic Cell 9* (8), 1150−8.

(3) Rovira-Graells, N., Gupta, A. P., Planet, E., Crowley, V. M., Mok, S., Ribas de Pouplana, L., Preiser, P. R., Bozdech, Z., and Cortes, A. (2012) Transcriptional variation in the malaria parasite Plasmodium falciparum. *Genome Res. 22* (5), 925−38.

(4) Flueck, C., Bartfai, R., Volz, J., Niederwieser, I., Salcedo-Amaya, A. M., Alako, B. T., Ehlgen, F., Ralph, S. A., Cowman, A. F., Bozdech, Z., Stunnenberg, H. G., and Voss, T. S. (2009) Plasmodium falciparum heterochromatin protein 1 marks genomic loci linked to phenotypic variation of exported virulence factors. *PLoS Pathog. 5* (9), e1000569.

(5) Lopez-Rubio, J. J., Mancio-Silva, L., and Scherf, A. (2009) Genome-wide analysis of heterochromatin associates clonally variant gene regulation with perinuclear repressive centers in malaria parasites. *Cell Host Microbe 5* (2), 179−90.

(6) Brancucci, N. M. B., Bertschi, N. L., Zhu, L., Niederwieser, I., Chin, W. H., Wampfler, R., Freymond, C., Rottmann, M., Felger, I., Bozdech, Z., and Voss, T. S. (2014) Heterochromatin protein 1 secures survival and transmission of malaria parasites. *Cell Host Microbe 16* (2), 165−176.

(7) Deitsch, K. W., and Dzikowski, R. (2017) Variant Gene Expression and Antigenic Variation by Malaria Parasites. *Annu. Rev. Microbiol. 71*, 625−641.

(8) Swamy, L., Amulic, B., and Deitsch, K. W. (2011) Plasmodium falciparum var gene silencing is determined by cis DNA elements that form stable and heritable interactions. *Eukaryotic Cell 10* (4), 530−9.

(9) Duraisingh, M. T., and Horn, D. (2016) Epigenetic Regulation of Virulence Gene Expression in Parasitic Protozoa. *Cell Host Microbe 19* (5), 629−40.

(10) Merrick, C. J., Huttenhower, C., Buckee, C., Amambua-Ngwa, A., Gomez-Escobar, N., Walther, M., Conway, D. J., and Duraisingh, M. T. (2012) Epigenetic dysregulation of virulence gene expression in severe Plasmodium falciparum malaria. *J. Infect. Dis. 205* (10), 1593−600.

(11) Jiang, L., Lopez-Barragan, M. J., Jiang, H., Mu, J., Gaur, D., Zhao, K., Felsenfeld, G., and Miller, L. H. (2010) Epigenetic control of the variable expression of a Plasmodium falciparum receptor protein for erythrocyte invasion. *Proc. Natl. Acad. Sci. U. S. A. 107* (5), 2224−9.

(12) Markolovic, S., Leissing, T. M., Chowdhury, R., Wilkins, S. E., Lu, X., and Schofield, C. J. (2016) Structure-function relationships of human JmjC oxygenases-demethylases versus hydroxylases. *Curr. Opin. Struct. Biol. 41*, 62−72.

(13) Herr, C. Q., and Hausinger, R. P. (2018) Amazing Diversity in Biochemical Roles of Fe(II)/2-Oxoglutarate Oxygenases. *Trends Biochem. Sci. 43* (7), 517−532.

(14) Cui, L. W., Fan, Q., Cui, L., and Miao, J. (2008) Histone lysine methyltransferases and demethylases in Plasmodium falciparum. *Int. J. Parasitol. 38* (10), 1083−1097.

(15) Jiang, L., Mu, J., Zhang, Q., Ni, T., Srinivasan, P., Rayavara, K., Yang, W., Turner, L., Lavstsen, T., Theander, T. G., Peng, W., Wei, G., Jing, Q., Wakabayashi, Y., Bansal, A., Luo, Y., Ribeiro, J. M., Scherf, A., Aravind, L., Zhu, J., Zhao, K., and Miller, L. H. (2013) PfSETvs methylation of histone H3K36 represses virulence genes in Plasmodium falciparum. *Nature 499* (7457), 223−7.

(16) Aurrecoechea, C., Brestelli, J., Brunk, B. P., Dommer, J., Fischer, S., Gajria, B., Gao, X., Gingle, A., Grant, G., Harb, O. S., Heiges, M., Innamorato, F., Iodice, J., Kissinger, J. C., Kraemer, E., Li, W., Miller, J. A., Nayak, V., Pennington, C., Pinney, D. F., Roos, D. S., Ross, C., Stoeckert, C. J., Jr., Treatman, C., and Wang, H. (2009) PlasmoDB: a functional genomic database for malaria parasites. *Nucleic Acids Res. 37* (Database), D539−D543.

(17) Bartfai, R., Hoeijmakers, W. A., Salcedo-Amaya, A. M., Smits, A. H., Janssen-Megens, E., Kaan, A., Treeck, M., Gilberger, T. W., Francoijs, K. J., and Stunnenberg, H. G. (2010) H2A.Z demarcates intergenic regions of the plasmodium falciparum epigenome that are

dynamically marked by H3K9ac and H3K4me3. *PLoS Pathog. 6* (12), e1001223.
(18) Lopez-Barragan, M. J., Lemieux, J., Quinones, M., Williamson, K. C., Molina-Cruz, A., Cui, K., Barillas-Mury, C., Zhao, K., and Su, X. Z. (2011) Directional gene expression and antisense transcripts in sexual and asexual stages of Plasmodium falciparum. *BMC Genomics 12*, 587.
(19) Young, J. A., Fivelman, Q. L., Blair, P. L., de la Vega, P., Le Roch, K. G., Zhou, Y., Carucci, D. J., Baker, D. A., and Winzeler, E. A. (2005) The Plasmodium falciparum sexual development transcriptome: a microarray analysis using ontology-based pattern identification. *Mol. Biochem. Parasitol. 143* (1), 67−79.
(20) Zhang, M., Wang, C., Otto, T. D., Oberstaller, J., Liao, X., Adapa, S. R., Udenze, K., Bronner, I. F., Casandra, D., Mayho, M., Brown, J., Li, S., Swanson, J., Rayner, J. C., Jiang, R. H. Y., and Adams, J. H. (2018) Uncovering the essential genes of the human malaria parasite Plasmodium falciparum by saturation mutagenesis. *Science 360* (6388), eaap7847.
(21) Hojfeldt, J. W., Agger, K., and Helin, K. (2013) Histone lysine demethylases as targets for anticancer therapy. *Nat. Rev. Drug Discovery 12* (12), 917−30.
(22) Maes, T., Carceller, E., Salas, J., Ortega, A., and Buesa, C. (2015) Advances in the development of histone lysine demethylase inhibitors. *Curr. Opin. Pharmacol. 23*, 52−60.
(23) Wang, L., Chang, J., Varghese, D., Dellinger, M., Kumar, S., Best, A. M., Ruiz, J., Bruick, R., Pena-Llopis, S., Xu, J., Babinski, D. J., Frantz, D. E., Brekken, R. A., Quinn, A. M., Simeonov, A., Easmon, J., and Martinez, E. D. (2013) A small molecule modulates Jumonji histone demethylase activity and selectively inhibits cancer growth. *Nat. Commun. 4*, 2035.
(24) Bayo, J., Dalvi, M. P., and Martinez, E. D. (2015) Successful strategies in the discovery of small-molecule epigenetic modulators with anticancer potential. *Future Med. Chem. 7* (16), 2243−61.
(25) Cascella, B., Lee, S. G., Singh, S., Jez, J. M., and Mirica, L. M. (2017) The small molecule JIB-04 disrupts O2 binding in the Fe-dependent histone demethylase KDM4A/JMJD2A. *Chem. Commun. (Cambridge, U. K.) 53* (13), 2174−2177.
(26) Horton, J. R., Liu, X., Gale, M., Wu, L., Shanks, J. R., Zhang, X., Webber, P. J., Bell, J. S., Kales, S. C., Mott, B. T., Rai, G., Jansen, D. J., Henderson, M. J., Urban, D. J., Hall, M. D., Simeonov, A., Maloney, D. J., Johns, M. A., Fu, H., Jadhav, A., Vertino, P. M., Yan, Q., and Cheng, X. (2016) Structural Basis for KDM5A Histone Lysine Demethylase Inhibition by Diverse Compounds. *Cell Chem. Biol. 23* (7), 769−81.
(27) Kruidenier, L., Chung, C. W., Cheng, Z., Liddle, J., Che, K., Joberty, G., Bantscheff, M., Bountra, C., Bridges, A., Diallo, H., Eberhard, D., Hutchinson, S., Jones, E., Katso, R., Leveridge, M., Mander, P. K., Mosley, J., Ramirez-Molina, C., Rowland, P., Schofield, C. J., Sheppard, R. J., Smith, J. E., Swales, C., Tanner, R., Thomas, P., Tumber, A., Drewes, G., Oppermann, U., Patel, D. J., Lee, K., and Wilson, D. M. (2012) A selective jumonji H3K27 demethylase inhibitor modulates the proinflammatory macrophage response. *Nature 488* (7411), 404−8.
(28) Thinnes, C. C., England, K. S., Kawamura, A., Chowdhury, R., Schofield, C. J., and Hopkinson, R. J. (2014) Targeting histone lysine demethylases - progress, challenges, and the future. *Biochim. Biophys. Acta, Gene Regul. Mech. 1839* (12), 1416−32.
(29) Vinogradova, M., Gehling, V. S., Gustafson, A., Arora, S., Tindell, C. A., Wilson, C., Williamson, K. E., Guler, G. D., Gangurde, P., Manieri, W., Busby, J., Flynn, E. M., Lan, F., Kim, H. J., Odate, S., Cochran, A. G., Liu, Y., Wongchenko, M., Yang, Y., Cheung, T. K., Maile, T. M., Lau, T., Costa, M., Hegde, G. V., Jackson, E., Pitti, R., Arnott, D., Bailey, C., Bellon, S., Cummings, R. T., Albrecht, B. K., Harmange, J. C., Kiefer, J. R., Trojer, P., and Classon, M. (2016) An inhibitor of KDM5 demethylases reduces survival of drug-tolerant cancer cells. *Nat. Chem. Biol. 12* (7), 531−8.
(30) Smilkstein, M., Sriwilaijaroen, N., Kelly, J. X., Wilairat, P., and Riscoe, M. (2004) Simple and Inexpensive Fluorescence-Based Technique for High-Throughput Antimalarial Drug Screening. *Antimicrob. Agents Chemother. 48* (5), 1803−1806.
(31) Ntziachristos, P., Tsirigos, A., Welstead, G. G., Trimarchi, T., Bakogianni, S., Xu, L., Loizou, E., Holmfeldt, L., Strikoudis, A., King, B., Mullenders, J., Becksfort, J., Nedjic, J., Paietta, E., Tallman, M. S., Rowe, J. M., Tonon, G., Satoh, T., Kruidenier, L., Prinjha, R., Akira, S., Van Vlierberghe, P., Ferrando, A. A., Jaenisch, R., Mullighan, C. G., and Aifantis, I. (2014) Contrasting roles of histone 3 lysine 27 demethylases in acute lymphoblastic leukaemia. *Nature 514* (7523), 513−7.
(32) Dalvi, M. P., Wang, L., Zhong, R., Kollipara, R. K., Park, H., Bayo, J., Yenerall, P., Zhou, Y., Timmons, B. C., Rodriguez-Canales, J., Behrens, C., Mino, B., Villalobos, P., Parra, E. R., Suraokar, M., Pataer, A., Swisher, S. G., Kalhor, N., Bhanu, N. V., Garcia, B. A., Heymach, J. V., Coombes, K., Xie, Y., Girard, L., Gazdar, A. F., Kittler, R., Wistuba, I. I., Minna, J. D., and Martinez, E. D. (2017) Taxane-Platin-Resistant Lung Cancers Co-develop Hypersensitivity to JumonjiC Demethylase Inhibitors. *Cell Rep. 19* (8), 1669−1684.
(33) Heinemann, B., Nielsen, J. M., Hudlebusch, H. R., Lees, M. J., Larsen, D. V., Boesen, T., Labelle, M., Gerlach, L. O., Birk, P., and Helin, K. (2014) Inhibition of demethylases by GSK-J1/J4. *Nature 514* (7520), E1−2.
(34) Hamada, S., Suzuki, T., Mino, K., Koseki, K., Oehme, F., Flamme, I., Ozasa, H., Itoh, Y., Ogasawara, D., Komaarashi, H., Kato, A., Tsumoto, H., Nakagawa, H., Hasegawa, M., Sasaki, R., Mizukami, T., and Miyata, N. (2010) Design, synthesis, enzyme-inhibitory activity, and effect on human cancer cells of a novel series of jumonji domain-containing protein 2 histone demethylase inhibitors. *J. Med. Chem. 53* (15), 5629−38.
(35) Cucchiara, V., Yang, J. C., Mirone, V., Gao, A. C., Rosenfeld, M. G., and Evans, C. P. (2017) Epigenomic Regulation of Androgen Receptor Signaling: Potential Role in Prostate Cancer Therapy. *Cancers 9* (1), 9.
(36) Johansson, C., Velupillai, S., Tumber, A., Szykowska, A., Hookway, E. S., Nowak, R. P., Strain-Damerell, C., Gileadi, C., Philpott, M., Burgess-Brown, N., Wu, N., Kopec, J., Nuzzi, A., Steuber, H., Egner, U., Badock, V., Munro, S., LaThangue, N. B., Westaway, S., Brown, J., Athanasou, N., Prinjha, R., Brennan, P. E., and Oppermann, U. (2016) Structural analysis of human KDM5B guides histone demethylase inhibitor development. *Nat. Chem. Biol. 12* (7), 539−45.
(37) Delves, M. J., Straschil, U., Ruecker, A., Miguel-Blanco, C., Marques, S., Dufour, A. C., Baum, J., and Sinden, R. E. (2016) Routine in vitro culture of P. falciparum gametocytes to evaluate novel transmission-blocking interventions. *Nat. Protoc. 11* (9), 1668−80.
(38) Ruecker, A., Mathias, D. K., Straschil, U., Churcher, T. S., Dinglasan, R. R., Leroy, D., Sinden, R. E., and Delves, M. J. (2014) A male and female gametocyte functional viability assay to identify biologically relevant malaria transmission-blocking drugs. *Antimicrob. Agents Chemother. 58* (12), 7292−302.
(39) Delves, M. J., Ruecker, A., Straschil, U., Lelievre, J., Marques, S., Lopez-Barragan, M. J., Herreros, E., and Sinden, R. E. (2013) Male and female Plasmodium falciparum mature gametocytes show different responses to antimalarial drugs. *Antimicrob. Agents Chemother. 57* (7), 3268−74.
(40) Hancock, R. L., Abboud, M. I., Smart, T. J., Flashman, E., Kawamura, A., Schofield, C. J., and Hopkinson, R. J. (2018) Lysine-241 Has a Role in Coupling 2OG Turnover with Substrate Oxidation During KDM4-Catalysed Histone Demethylation. *ChemBioChem 19* (9), 917−921.
(41) Lopez-Rubio, J. J., Gontijo, A. M., Nunes, M. C., Issar, N., Hernandez Rivas, R., and Scherf, A. (2007) 5′ flanking region of var genes nucleate histone modification patterns linked to phenotypic inheritance of virulence traits in malaria parasites. *Mol. Microbiol. 66* (6), 1296−1305.
(42) Chookajorn, T., Dzikowski, R., Frank, M., Li, F., Jiwani, A. Z., Hartl, D. L., and Deitsch, K. W. (2007) Epigenetic memory at malaria virulence genes. *Proc. Natl. Acad. Sci. U. S. A. 104* (3), 899−902.

(43) Karmodiya, K., Pradhan, S. J., Joshi, B., Jangid, R., Reddy, P. C., and Galande, S. (2015) A comprehensive epigenome map of Plasmodium falciparum reveals unique mechanisms of transcriptional regulation and identifies H3K36me2 as a global mark of gene suppression. *Epigenet. Chromatin 8*, 32.
(44) Ukaegbu, U. E., Kishore, S. P., Kwiatkowski, D. L., Pandarinath, C., Dahan-Pasternak, N., Dzikowski, R., and Deitsch, K. W. (2014) Recruitment of PfSET2 by RNA polymerase II to variant antigen encoding loci contributes to antigenic variation in P. falciparum. *PLoS Pathog. 10* (1), e1003854.
(45) Gupta, A. P., Chin, W. H., Zhu, L., Mok, S., Luah, Y. H., Lim, E. H., and Bozdech, Z. (2013) Dynamic epigenetic regulation of gene expression during the life cycle of malaria parasite Plasmodium falciparum. *PLoS Pathog. 9* (2), e1003170.
(46) Rai, R., Zhu, L., Chen, H., Gupta, A. P., Sze, S. K., Zheng, J., Ruedl, C., Bozdech, Z., and Featherstone, M. (2014) Genome-wide analysis in Plasmodium falciparum reveals early and late phases of RNA polymerase II occupancy during the infectious cycle. *BMC Genomics 15*, 959.
(47) Chaal, B. K., Gupta, A. P., Wastuwidyaningtyas, B. D., Luah, Y. H., and Bozdech, Z. (2010) Histone deacetylases play a major role in the transcriptional regulation of the Plasmodium falciparum life cycle. *PLoS Pathog. 6* (1), e1000737.
(48) Hu, G., Cabrera, A., Kono, M., Mok, S., Chaal, B. K., Haase, S., Engelberg, K., Cheemadan, S., Spielmann, T., Preiser, P. R., Gilberger, T. W., and Bozdech, Z. (2010) Transcriptional profiling of growth perturbations of the human malaria parasite Plasmodium falciparum. *Nat. Biotechnol. 28* (1), 91−8.
(49) Bozdech, Z., Llinas, M., Pulliam, B. L., Wong, E. D., Zhu, J., and DeRisi, J. L. (2003) The transcriptome of the intraerythrocytic developmental cycle of Plasmodium falciparum. *PLoS Biol. 1* (1), E5.
(50) Santos, J. M., Josling, G., Ross, P., Joshi, P., Orchard, L., Campbell, T., Schieler, A., Cristea, I. M., and Llinas, M. (2017) Red Blood Cell Invasion by the Malaria Parasite Is Coordinated by the PfAP2-I Transcription Factor. *Cell Host Microbe 21* (6), 731−741.E10.
(51) Josling, G. A., Petter, M., Oehring, S. C., Gupta, A. P., Dietz, O., Wilson, D. W., Schubert, T., Langst, G., Gilson, P. R., Crabb, B. S., Moes, S., Jenoe, P., Lim, S. W., Brown, G. V., Bozdech, Z., Voss, T. S., and Duffy, M. F. (2015) A Plasmodium Falciparum Bromodomain Protein Regulates Invasion Gene Expression. *Cell Host Microbe 17* (6), 741−51.
(52) Leykauf, K., Treeck, M., Gilson, P. R., Nebl, T., Braulke, T., Cowman, A. F., Gilberger, T. W., and Crabb, B. S. (2010) Protein kinase a dependent phosphorylation of apical membrane antigen 1 plays an important role in erythrocyte invasion by the malaria parasite. *PLoS Pathog. 6* (6), e1000941.
(53) Lasonder, E., Green, J. L., Camarda, G., Talabani, H., Holder, A. A., Langsley, G., and Alano, P. (2012) The Plasmodium falciparum schizont phosphoproteome reveals extensive phosphatidylinositol and cAMP-protein kinase A signaling. *J. Proteome Res. 11* (11), 5323−37.
(54) Lasonder, E., Rijpma, S. R., van Schaijk, B. C., Hoeijmakers, W. A., Kensche, P. R., Gresnigt, M. S., Italiaander, A., Vos, M. W., Woestenenk, R., Bousema, T., Mair, G. R., Khan, S. M., Janse, C. J., Bartfai, R., and Sauerwein, R. W. (2016) Integrated transcriptomic and proteomic analyses of P. falciparum gametocytes: molecular insight into sex-specific processes and translational repression. *Nucleic Acids Res. 44* (13), 6087−101.
(55) Modrzynska, K., Pfander, C., Chappell, L., Yu, L., Suarez, C., Dundas, K., Gomes, A. R., Goulding, D., Rayner, J. C., Choudhary, J., and Billker, O. (2017) A Knockout Screen of ApiAP2 Genes Reveals Networks of Interacting Transcriptional Regulators Controlling the Plasmodium Life Cycle. *Cell Host Microbe 21* (1), 11−22.
(56) Malmquist, N. A., Moss, T. A., Mecheri, S., Scherf, A., and Fuchter, M. J. (2012) Small-molecule histone methyltransferase inhibitors display rapid antimalarial activity against all blood stage forms in Plasmodium falciparum. *Proc. Natl. Acad. Sci. U. S. A. 109* (41), 16708−13.
(57) Malmquist, N. A., Sundriyal, S., Caron, J., Chen, P., Witkowski, B., Menard, D., Suwanarusk, R., Renia, L., Nosten, F., Jimenez-Diaz, M. B., Angulo-Barturen, I., Santos Martinez, M., Ferrer, S., Sanz, L. M., Gamo, F. J., Wittlin, S., Duffy, S., Avery, V. M., Ruecker, A., Delves, M. J., Sinden, R. E., Fuchter, M. J., and Scherf, A. (2015) Histone methyltransferase inhibitors are orally bioavailable, fast-acting molecules with activity against different species causing malaria in humans. *Antimicrob. Agents Chemother. 59* (2), 950−959.
(58) Sundriyal, S., Malmquist, N. A., Caron, J., Blundell, S., Liu, F., Chen, X., Srimongkolpithak, N., Jin, J., Charman, S. A., Scherf, A., and Fuchter, M. J. (2014) Development of Diaminoquinazoline Histone Lysine Methyltransferase Inhibitors as Potent Blood-Stage Antimalarial Compounds. *ChemMedChem 9*, 2360.
(59) Andrews, K. T., Gupta, A. P., Tran, T. N., Fairlie, D. P., Gobert, G. N., and Bozdech, Z. (2012) Comparative gene expression profiling of P. falciparum malaria parasites exposed to three different histone deacetylase inhibitors. *PLoS One 7* (2), e31847.
(60) Hansen, F. K., Sumanadasa, S. D., Stenzel, K., Duffy, S., Meister, S., Marek, L., Schmetter, R., Kuna, K., Hamacher, A., Mordmuller, B., Kassack, M. U., Winzeler, E. A., Avery, V. M., Andrews, K. T., and Kurz, T. (2014) Discovery of HDAC inhibitors with potent activity against multiple malaria parasite life cycle stages. *Eur. J. Med. Chem. 82*, 204−13.
(61) Marfurt, J., Chalfein, F., Prayoga, P., Wabiser, F., Kenangalem, E., Piera, K. A., Fairlie, D. P., Tjitra, E., Anstey, N. M., Andrews, K. T., and Price, R. N. (2011) Ex vivo activity of histone deacetylase inhibitors against multidrug-resistant clinical isolates of Plasmodium falciparum and P. vivax. *Antimicrob. Agents Chemother. 55* (3), 961−6.
(62) Sumanadasa, S. D., Goodman, C. D., Lucke, A. J., Skinner-Adams, T., Sahama, I., Haque, A., Do, T. A., McFadden, G. I., Fairlie, D. P., and Andrews, K. T. (2012) Antimalarial activity of the anticancer histone deacetylase inhibitor SB939. *Antimicrob. Agents Chemother. 56* (7), 3849−56.
(63) Trenholme, K., Marek, L., Duffy, S., Pradel, G., Fisher, G., Hansen, F. K., Skinner-Adams, T. S., Butterworth, A., Ngwa, C. J., Moecking, J., Goodman, C. D., McFadden, G. I., Sumanadasa, S. D., Fairlie, D. P., Avery, V. M., Kurz, T., and Andrews, K. T. (2014) Lysine acetylation in sexual stage malaria parasites is a target for antimalarial small molecules. *Antimicrob. Agents Chemother. 58* (7), 3666−78.
(64) Salcedo-Amaya, A. M., van Driel, M. A., Alako, B. T., Trelle, M. B., van den Elzen, A. M., Cohen, A. M., Janssen-Megens, E. M., van de Vegte-Bolmer, M., Selzer, R. R., Iniguez, A. L., Green, R. D., Sauerwein, R. W., Jensen, O. N., and Stunnenberg, H. G. (2009) Dynamic histone H3 epigenome marking during the intraerythrocytic cycle of Plasmodium falciparum. *Proc. Natl. Acad. Sci. U. S. A. 106* (24), 9655−60.
(65) Hoeijmakers, W. A., Salcedo-Amaya, A. M., Smits, A. H., Francoijs, K. J., Treeck, M., Gilberger, T. W., Stunnenberg, H. G., and Bartfai, R. (2013) H2A.Z/H2B.Z double-variant nucleosomes inhabit the AT-rich promoter regions of the Plasmodium falciparum genome. *Mol. Microbiol. 87* (5), 1061−73.
(66) Coetzee, N., Sidoli, S., van Biljon, R., Painter, H., Llinas, M., Garcia, B. A., and Birkholtz, L. M. (2017) Quantitative chromatin proteomics reveals a dynamic histone post-translational modification landscape that defines asexual and sexual Plasmodium falciparum parasites. *Sci. Rep. 7* (1), 607.
(67) Pinskaya, M., and Morillon, A. (2009) Histone H3 lysine 4 di-methylation: a novel mark for transcriptional fidelity? *Epigenetics 4* (5), 302−6.
(68) Kafsack, B. F., Rovira-Graells, N., Clark, T. G., Bancells, C., Crowley, V. M., Campino, S. G., Williams, A. E., Drought, L. G., Kwiatkowski, D. P., Baker, D. A., Cortes, A., and Llinas, M. (2014) A transcriptional switch underlies commitment to sexual development in malaria parasites. *Nature 507* (7491), 248−52.
(69) Jin, C., Yang, L., Xie, M., Lin, C., Merkurjev, D., Yang, J. C., Tanasa, B., Oh, S., Zhang, J., Ohgi, K. A., Zhou, H., Li, W., Evans, C. P., Ding, S., and Rosenfeld, M. G. (2014) Chem-seq permits identification of genomic targets of drugs against androgen receptor

https://dx.doi.org/10.1021/acsinfecdis.9b00455
ACS Infect. Dis. 2020, 6, 1058−1075

regulation selected by functional phenotypic screens. *Proc. Natl. Acad. Sci. U. S. A. 111* (25), 9235−40.
(70) Zhang, X., Huang, Y., and Shi, X. (2015) Emerging roles of lysine methylation on non-histone proteins. *Cell. Mol. Life Sci. 72* (22), 4257−72.
(71) Iyer, L. M., Abhiman, S., de Souza, R. F., and Aravind, L. (2010) Origin and evolution of peptide-modifying dioxygenases and identification of the wybutosine hydroxylase/hydroperoxidase. *Nucleic Acids Res. 38* (16), 5261−79.
(72) Markolovic, S., Zhuang, Q., Wilkins, S. E., Eaton, C. D., Abboud, M. I., Katz, M. J., McNeil, H. E., Lesniak, R. K., Hall, C., Struwe, W. B., Konietzny, R., Davis, S., Yang, M., Ge, W., Benesch, J. L. P., Kessler, B. M., Ratcliffe, P. J., Cockman, M. E., Fischer, R., Wappner, P., Chowdhury, R., Coleman, M. L., and Schofield, C. J. (2018) The Jumonji-C oxygenase JMJD7 catalyzes (3S)-lysyl hydroxylation of TRAFAC GTPases. *Nat. Chem. Biol. 14* (7), 688−695.
(73) Wilkins, S. E., Islam, M. S., Gannon, J. M., Markolovic, S., Hopkinson, R. J., Ge, W., Schofield, C. J., and Chowdhury, R. (2018) JMJD5 is a human arginyl C-3 hydroxylase. *Nat. Commun. 9* (1), 1180.
(74) Markolovic, S., Wilkins, S. E., and Schofield, C. J. (2015) Protein Hydroxylation Catalyzed by 2-Oxoglutarate-dependent Oxygenases. *J. Biol. Chem. 290* (34), 20712−22.
(75) Trager, W., and Jensen, J. B. (1997) Continuous culture of Plasmodium falciparum: its impact on malaria research. *Int. J. Parasitol. 27* (9), 989−1006.
(76) McLean, K. J., Straimer, J., Hopp, C. S., Vega-Rodriguez, J., Small-Saunders, J. L., Kanatani, S., Tripathi, A., Mlambo, G., Dumoulin, P. C., Harris, C. T., Tong, X., Shears, M. J., Ankarklev, J., Kafsack, B. F. C., Fidock, D. A., and Sinnis, P. (2019) Generation of Transgenic Human Malaria Parasites With Strong Fluorescence in the Transmission Stages. *Sci. Rep. 9*, 13131.
(77) Fivelman, Q. L., McRobert, L., Sharp, S., Taylor, C. J., Saeed, M., Swales, C. A., Sutherland, C. J., and Baker, D. A. (2007) Improved synchronous production of Plasmodium falciparum gametocytes in vitro. *Mol. Biochem. Parasitol. 154* (1), 119−23.
(78) Grimberg, B. T. (2011) Methodology and application of flow cytometry for investigation of human malaria parasites. *J. Immunol. Methods 367* (1−2), 1−16.
(79) Muench, S. P., Rafferty, J. B., McLeod, R., Rice, D. W., and Prigge, S. T. (2003) Expression, purification and crystallization of the Plasmodium falciparum enoyl reductase. *Acta Crystallogr., Sect. D: Biol. Crystallogr. 59* (Pt7), 1246−1248.
(80) Bhanu, N. V., Sidoli, S., and Garcia, B. A. (2016) Histone modification profiling reveals differential signatures associated with human embryonic stem cell self-renewal and differentiation. *Proteomics 16* (3), 448−58.
(81) Sidoli, S., Bhanu, N. V., Karch, K. R., Wang, X., and Garcia, B. A. (2016) Complete Workflow for Analysis of Histone Post-translational Modifications Using Bottom-up Mass Spectrometry: From Histone Extraction to Data Analysis. *J. Visualized Exp.* No. 111, e54112.
(82) Robinson, M. D., McCarthy, D. J., and Smyth, G. K. (2010) edgeR: a Bioconductor package for differential expression analysis of digital gene expression data. *Bioinformatics 26* (1), 139−40.
(83) McCarthy, D. J., Chen, Y., and Smyth, G. K. (2012) Differential expression analysis of multifactor RNA-Seq experiments with respect to biological variation. *Nucleic Acids Res. 40* (10), 4288−97.
(84) Hulsen, T., de Vlieg, J., and Alkema, W. (2008) BioVenn - a web application for the comparison and visualization of biological lists using area-proportional Venn diagrams. *BMC Genomics 9*, 488.

https://dx.doi.org/10.1021/acsinfecdis.9b00455
ACS Infect. Dis. 2020, 6, 1058−1075